SYSTEMATIC INVESTIGATIONS FOR INDUSTRIAL DEVELOPMENT

EDITOR
Assist. Prof. Serkan GÜLDAL

İKSAD
Publishing House

SYSTEMATIC INVESTIGATIONS FOR INDUSTRIAL DEVELOPMENT

EDITOR

Assist. Prof. Serkan GÜLDAL

AUTHORS

Prof. Dr. Yağmur UYSAL

Prof. Dr. Yusuf URAS

Assist. Prof. Aslı BORU İPEK

Assist. Prof. Hasan Üstün BAŞARAN

Dr. Begümhan TURGUT

Dr. Cihan YALÇIN

Dr. Ethem İlhan ŞAHİN

Beyza Begüm TUFAN

Selim Burak CANTÜRK

Volkan DALYAN, MSc.

İKSAD Publishing House

(The Licence Number of Publicator: 2014/31220)
TURKEY TR: +90 342 606 06 75
USA: +1 631 685 0 853
E mail: iksadyayinevi@gmail.com
www.iksadyayinevi.com

ISBN: 978-625-367-000-9
Cover Design: İbrahim KAYA
March / 2023
Ankara / Turkey
Size = 16x24 cm

CONTENTS

CHAPTER 5

CORROSION PROPERTIES OF CuSnSi ALLOY IN DIFFERENT MEDIUMS

PREFACE

Industrial developments have significant effects on society. Besides to economic impact, it correlates with life quality. To contribute industrial development, numerous methods are introduced to improve production or reduce the cost in this book. The chapters are collected about the studies which subject from material durability to locating the production facility. The experts of the fields share their investigations. To provide an enjoyable reading experience, the book language avoids technical terminology.

The five chapters cover various problems with the proposed solutions. In the first chapter, the durability properties of CuSnSi are investigated by experimental methods. Although a specific alloy is given, the applied method can be used for different alloys. The properties are tested for different circumstances, and the chapter is titled as *"Corrosion Properties of CuSnSi Alloy in Different Mediums."* In the second chapter, system engineering methods are presented to place a paper recycling plant. The chapter is titled as *"A Hybrid Fuzzy AHP And VIKOR Method for Facility Location Selection in A Paper Recycling Plant."* In the third chapter, researchers are tested engine performance by different methods in silico. The chapter concludes that the combination of the methods provide better results, and it is titled *"Implementing Late Exhaust Valve Opening and Internal Exhaust Gas Recirculation to Improve Diesel Exhaust System Warm Up in Automotives Marine Vehicles."* In chapter four, different approaches are discussed for mobile agent discovery, and it is presented with the title *"Overview of Service Discovery Using Clustering with Mobile Agents."* In chapter five, drinking water analysis are provided with local examples. The chapter is titled *"Hydrogeochemistry of the Drinking Water Sources of the Büyükkizilcik Region (Kahramanmaraş, Turkey)."* For the chapters, all responsibilities for the provided content belong to the authors.

We are grateful to authors' contribution to this book and ISPEC publishing house. We hope this book provides systematic investigations from basic knowledge to deeper understanding.

Assist. Prof. Serkan Güldal

March 2023

CHAPTER 1

A HYBRID FUZZY AHP AND VIKOR METHOD FOR FACILITY LOCATION SELECTION IN A PAPER RECYCLING PLANT

Beyza Begüm TUFAN[1]

Asst. Prof. Dr. Aslı BORU İPEK[2]

[1] Adana Alparslan Türkeş Science and Technology University, Industrial Engineering Department, begum_tufan@hotmail.com
[2] Kütahya Dumlupınar University, Management Information Systems Department, asli.ipek@dpu.edu.tr

INTRODUCTION

Companies are forced to reduce costs of globalization and the current competitive environment. The location of production and service operations has a significant impact on price and operating costs. Deciding where to locate a facility is the first step in the struggle to cut costs. For these reasons, choosing a facility location that is expensive and extremely difficult to change quickly is a crucial decision for companies (Dag & Önder, 2013). Melo, Nickel, and Saldanha-Da-Gama (2009) examined the general relationship between facility location models and strategic supply chain planning. Decision-making on the location of the facility is an essential part of strategic planning for many different private and public companies. Decision-makers must select locations that will not only function well in the current system state but also remain profitable over the facility's lifetime, regardless of changes in the environment, population shifts, and market trends (Owen & Daskin, 1998). Long-term decisions affect the company's operations and require for in-depth understanding of the company and its environment (Thanh, Bostel, & Péton, 2008).

Decisions about the location of the facility and its relocation are crucial managerial choices in modern supply chains. Managers encounter uncertainties and risks in this environment when making decisions (Sundarakani, Pereira, & Ishizaka, 2021). The inputs to traditional facility location models, such as costs, demands, travel times, and other factors, may be highly uncertain. For many years, researchers have been creating models for facility location in an uncertain environment (Snyder, 2006).

The optimal location generates greater economic benefits due to higher productivity and an efficient distribution system. When choosing between multiple alternative facility locations, it's important to compare each location's performance characteristics in a comprehensive way. Different multi-criteria decision-making (MCDM) methods can be successfully employed to address this type of problem because the facility location selection problem contains multiple conflicting criteria and a limited number of probable candidate alternatives (Chakraborty, Ray, & Dan, 2013). In this paper, a hybrid MCDM method including Fuzzy Analytical Hierarchy Process (FAHP) and Vise Kriterijumska Optimizacija I Kompromisno Resenje (VIKOR) is created to determine the suitable location of the paper recycling plant.

LITERATURE REVIEW

MCDM methods are effectively and frequently used at several planning stages, including supplier selection, investment project evaluation, workforce planning, and location selection. Decisions on the facility location require significant capital investment and create long-term restrictions on the production and distribution of goods (Yeşilkaya, 2018). In literature, various studies are available related to MCDM methods in facility location. For example, Yeşilkaya (2018) determined the paper factory location using Analytical Hierarchy Process (AHP), Technique for Order Preference by Similarity to Ideal Solution (TOPSIS), and preference ranking organization method for enrichment evaluations. In the study, a decision support model was proposed to determine the most suitable place among the five candidate cities. Aydemir-Karadağ (2019) applied the AHP and goal programming methods based on environmental, economic, social, and geological factors for solid waste storage facility site selection. İnağ and Arıkan (2020) determined the criteria affecting the location selection for solid waste dropping center and used a decision-making trial and evaluation laboratory to define the relationships between these criteria. Then, criteria weights and priority values of candidate facility locations were defined by the analytic network process method. Then, the site selection problem was modeled on the basis of p-median and p-centre models. The objective functions were combined with the determined priority values using the LP-metric approach, so the facility locations were determined as multi-objective. Bilgilioğlu and Gezgin (2022) used geographic information systems and FAHP. By evaluating all criteria, a suitability map for solid waste disposal areas in Nevşehir was produced, and candidate areas for the new facility were determined.

In literature, FAHP and VIKOR are used successfully in solving many different problems (Malviya & Kant, 2018; Wang, Nguyen, Dang, & Lu, 2021; Otay & Kahraman, 2022; Guo & Wu, 2022). Some of the previous studies on AHP, FAHP, and VIKOR are summarized below. Dag and Önder (2013) used data from a well-known label manufacturing company in Turkey to illustrate the facility location selection process. Using the AHP and VIKOR methods, the facility location selection was presented. Şişman (2017) presented a risk assessment in the automotive auxiliary industry by using FAHP and fuzzy VIKOR methods in the analysis of error types and effects. With the FAHP method, the significance of risk factors was firstly assessed in the study. The identified failure modes' risk priority was then ranked using the

fuzzy VIKOR method. Saraçoğlu and Dağıstanlı (2017) solved the supplier selection problem using FAHP and VIKOR methods. To solve the problem, the weights of the criteria were firstly determined with FAHP, and by using these weights, the order of preference to evaluate alternative suppliers was determined with the VIKOR method.

Parhizgarsharif, Lork, and Telvari (2019) proposed a new hybrid method. Firstly, the best worst method was employed to determine the weights of the selected criteria. After that, two gray relational analysis and VIKOR methodologies were employed to determine the final ranking of the locations. Gul (2020) suggested a novel method for risk assessment considering pythagorean FAHP and fuzzy VIKOR. Ayyildiz and Taskin (2022) utilized spherical fuzzy VIKOR and spherical FAHP. In the study, the criteria for selecting the petrol station(s) to serve during the lockdown were defined using a hierarchical criteria structure.

In this paper, FAHP and VIKOR are used to select the most appropriate paper recycling plant. The weights of each criterion are computed using FAHP, and then VIKOR method is utilized to rank the alternatives in order of best to worst.

PROPOSED METHODS

In this chapter, the company consists of a treatment plant, a power plant, a biogas plant, a pulp preparation plant, and a paper production plant. The company supplies products to many sectors from the paper industry to the textile industry. Products are sized according to the demands of the customers. The plant produces its products with 100% recycling.

The company wants to open a new recycling plant. This study aims to help the decision-makers in choosing the most suitable region by applying the methods of FAHP and VIKOR to select a new paper recycling plant location. With the help of previous studies (e.g., Güler & Yomralıoğlu, 2017; Şengün, Siler, & Engin, 2018; Yeşilkaya, 2018; Aydemir-Karadağ, 2019; and İnağ & Arıkan, 2020) and experts in this field, main criteria and sub-criteria to be used in this study are firstly determined. The proposed hybrid methodology is given in Figure 1.

In Table 1, six main criteria and 14 sub-criteria are given. The scoring was made by the expert working in the company considering four alternative recycling plant locations.

Table 1. Table of main criteria and sub-criteria.

Main Criteria	**Sub-Criteria**
Market	Demand
	Proximity of markets
	Sales prices
Labor	Workforce level
	Labor wages
Transportation	Easy access
	Transition density
Distance to Strategic Locations	Proximity to industrial zone
	Windbreakers cost
Climate Conditions	Wind domination
	Fire incidents
Land	Space usage
	Proximity to waste
	Road quality

The act of decision-making involves identifying and selecting alternatives from a range of options to determine the optimal action to take while taking the decision-maker's expectations into account. The diversity of criteria used to evaluate the alternatives is the decision-making process's most challenging element. MCDM stands for making decisions while dealing with multiple criteria. The advantage of MCDM is that it offers a fair assessment of how appropriate each alternative is. Additionally, it prevents one component from overpowering others (Chatterjee & Chakraborty, 2016).

AHP is one of the most widely used MCDM methods that use pairwise comparison to structurally calculate the weights of criteria and priorities of alternatives. Fuzzy sets can be integrated with AHP because comparisons based on subjective assessments may be imprecise. In many situations where it is necessary to carry out criteria prioritization and

alternative selection, FAHP has grown in significance (Sakhardande & Gaonkar, 2022). The FAHP uses a triangular fuzzy numbers scale (Chang, 1996).

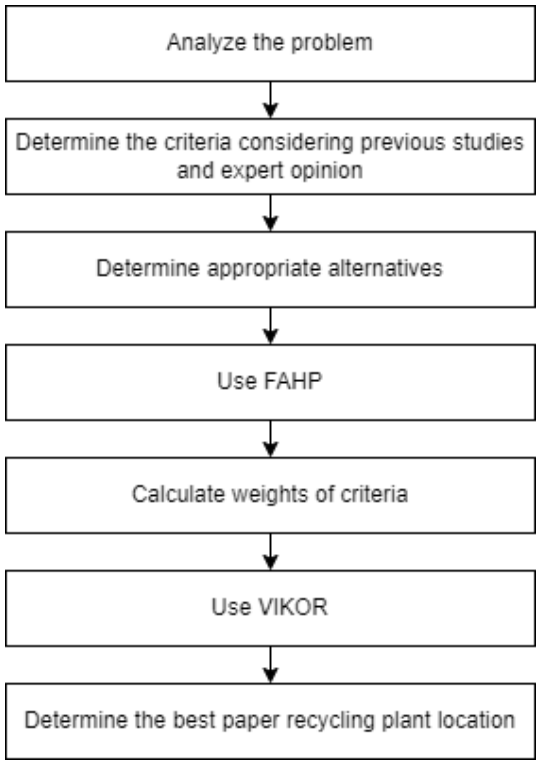

Figure 1. The proposed methodology.

Two well-known MCDM methods, FAHP and VIKOR, are integrated in this study. To support the decision-maker, VIKOR concentrates on selecting and ranking from a list of feasible alternatives and identifying a compromise solution for a problem with conflicting criteria. Based on the specific measure of closeness to the ideal solution, it generates the compromise ranking list (Chatterjee & Chakraborty, 2016). The fact that VIKOR uses linear normalization gives it an edge over other approaches, most notably TOPSIS. Thus, the VIKOR normalized values are independent of the criteria measurement unit (Eydi, Farughi, & Abdi, 2016).

RESULTS AND DISCUSSION

In this paper, FAHP is used to determine each criterion's weight, and the VIKOR method is suggested to prioritize alternatives from best to worst. Firstly, comparisons are made for the determined criteria, and a comparison matrix is created to show the importance of the criteria relative to each other. Comparison values of main criteria (MC) including market (1), labor (2), transportation (3), distance to strategic locations (4), climate conditions (5), and land (6) are given in Table 2. The most important criteria were determined as market (0.35), distance to strategic locations (0.261), climate conditions (0.176), land (0.098), labor (0.073), and transportation (0.042), respectively.

Table 2. Comparison values of main criteria (MC).

MC	1	2	3	4	5	6
1	(1,1,1)	(1,3,5)	(3,5,7)	(1,3,5)	(3,5,7)	(1,3,5)
2	(1/5,1/3,1/1)	(1,1,1)	(5,7,9)	(1/5,1/3,1/1)	(1/7,1/5,1/3)	(1/9,1/7,1/5)
3	(1/7,1/5,1/3)	(1/9,1/7,1/5)	(1,1,1)	(1/7,1/5,1/3)	(1/5,1/3,1/1)	(1/5,1/3,1/1)
4	(1/5,1/3,1/1)	(1,3,5)	(3,5,7)	(1,1,1)	(1,3,5)	(3,5,7)
5	(1/7,1/5,1/3)	(3,5,7)	(1,3,5)	(1/5,1/3,1/1)	(1,1,1)	(5,7,9)
6	(1/5,1/3,1/1)	(5,7,9)	(1,3,5)	(1/7,1/5,1/3)	(1/9,1/7,1/5)	(1,1,1)

The following is a description of the procedure used in the FAHP method. According to the criteria, the problem is defined. After, a comparison matrix is created. The chosen matrix is straightforward, supports the consistency framework well, gathers additional data that might be needed for all possible comparisons, and can examine the overall priority sensitivity for changes under consideration. After that, consistency is checked. Then, a triangular fuzzy number is set up, and the weight value of the fuzzy vector is calculated. Finally, alternatives are ranked and selected. Details about the application steps of FAHP can be found in Putra, Andryana, Fauziah, and Gunaryati (2018).

The procedure above is used to calculate the weight of each criterion in this study, and the VIKOR method is employed to determine the priority order of the alternatives. The steps of VIKOR can be summarized as follows. A comparison matrix is created to assess all alternatives based on a number of

criteria. The criteria weight vector can be calculated using various techniques depending on the weight and importance of various criteria in the decision-making process. Here FAHP is utilized to determine the weight of criteria. Then, the best and worst alternatives are identified for each criterion. The distance between alternatives and the ideal solution is calculated, and the VIKOR index is computed. Finally, alternatives are ranked, and the best alternative is selected. Details about the application steps of VIKOR can be found in Eydi et al. (2016).

The most appropriate alternative plant location was selected from four alternative regions. The result of the proposed hybrid FAHP-VIKOR method is alternative plant location 2, alternative plant location 1, alternative plant location 3, and alternative plant location 4, respectively. Thus, alternative plant location 2 is the best when compared with other alternatives.

CONCLUSION

FAHP and VIKOR are two of the most comprehensive and practical MCDM methods. These methods analyze complex problems, simplify them to a manageable size, and then resolve them. In this study, the weights obtained as a result of the FAHP are used in the VIKOR method. The selection is made from four alternatives.

Because of the uncertainty, facility location selection is now thought to be an extremely challenging topic. It was attempted to reduce this uncertainty by applying the FAHP-VIKOR method in the decision-making process. FAHP is used to add linguistic variables to the data, ensuring that comparison errors are minimized. The hybrid FAHP-VIKOR method will make it easier for the decision maker to quantitatively evaluate options in accordance with their predetermined criteria. The results of this study showed that alternative plant location 2 is the best when compared with other alternatives. In future studies, simulation can be applied to convert fuzzy numbers to non-fuzzy numbers. Other MCDM methods can be used to compare the results of FAHP-VIKOR.

REFERENCES

Aydemir-Karadağ, A. (2019). A combined goal programming and AHP Approach for solid waste landfill site selection. *International Journal of Engineering Research and Development*, *11* (1), 211-225.

Ayyildiz, E., & Taskin, A. (2022). A novel spherical fuzzy AHP-VIKOR methodology to determine serving petrol station selection during COVID-19 lockdown: A pilot study for İstanbul. *Socio-Economic Planning Sciences*, *83*, 101345.

Bilgilioğlu, S. S., & Gezgin, C. (2022). Suitable site selection for landfill with the integration of Geographic Information Systems (GIS) and Fuzzy Analytical Hierarchy Process (FAHP) methods in Nevşehir. *Afyon Kocatepe University Journal of Science and Engineering*, *22*(4), 836-849.

Chakraborty, R., Ray, A., & Dan, P. K. (2013). Multi criteria decision making methods for location selection of distribution centers. *International Journal of Industrial Engineering Computations*, *4*(4), 491-504.

Chang, D.-Y. (1996). Applications of the extent analysis method on fuzzy AHP. *European Journal of Operational Research*, *95*(3), 649-655.

Chatterjee, P., & Chakraborty, S. (2016). A comparative analysis of VIKOR method and its variants. *Decision Science Letters*, *5*(4), 469-486.

Dag, S., & Önder, E. (2013). Decision-making for facility location using VIKOR method. *Journal of International Scientific Publications: Economy & Business*, *7*(1), 308-330.

Eydi, A., Farughi, H., & Abdi, F. (2016). A hybrid method based on fuzzy AHP and VIKOR for the discrete time-cost-quality trade-off problem. *Journal of Optimization in Industrial Engineering*, *19*, 105-116.

Gul, M. (2020). Application of Pythagorean fuzzy AHP and VIKOR methods in occupational health and safety risk assessment: the case of a gun and rifle barrel external surface oxidation and colouring unit. *International Journal of Occupational Safety and Ergonomics*, *26*(4), 705-718.

Guo, R., & Wu, Z. (2022). Social sustainable supply chain performance assessment using hybrid fuzzy-AHP–DEMATEL–VIKOR: a case study in manufacturing enterprises. *Environment, Development and Sustainability*, 1-29. https://doi.org/10.1007/s10668-022-02565-3.

Güler, D., & Yomralıoğlu, T. (2017). Alternative suitable landfill site selection using analytic hierarchy process and geographic information

systems: a case study in Istanbul. *Environmental Earth Sciences*, *76*, 678.

İnağ, T. D., & Arikan, M. (2020). An integrated approach by DEMATEL-ANP and mathematical programming methods for site selection of solid waste dropping center: an application in Ankara Province. *Erciyes University Journal of Institue of Science and Technology*, *36*(1), 33-46.

Malviya, R. K., & Kant, R. (2018). Prioritising the solutions to overcome the barriers of green supply chain management implementation: a hybrid fuzzy AHP-VIKOR framework approach. *Journal of Decision Systems*, *27*(4), 275-320.

Melo, M. T., Nickel, S., & Saldanha-Da-Gama, F. (2009). Facility location and supply chain management–A review. *European Journal of Operational Research*, *196*(2), 401-412.

Otay, İ., & Kahraman, C. (2022). A novel circular intuitionistic fuzzy AHP&VIKOR methodology: An application to a multi-expert supplier evaluation problem. *Pamukkale University Journal of Engineering Sciences*, *28*(1), 194-207.

Owen, S. H., & Daskin, M. S. (1998). Strategic facility location: A review. *European Journal of Operational Research*, *111*(3), 423-447.

Parhizgarsharif, A., Lork, A., & Telvari, A. (2019). A hybrid approach based on the BWM-VIKOR and GRA for ranking facility location in construction site layout for Mehr project in Tehran. *Decision Science Letters*, *8*(3), 233-248.

Putra, M. S. D., Andryana, S., Fauziah, & Gunaryati, A. (2018). Fuzzy analytical hierarchy process method to determine the quality of gemstones. *Advances in Fuzzy Systems*, Article ID 9094380, 6 pages, https://doi.org/10.1155/2018/9094380

Sakhardande, M. J., & Gaonkar, R. S. P. (2022). On solving large data matrix problems in Fuzzy AHP. *Expert Systems with Applications*, *194*, 116488.

Saraçoğlu, İ., & Dağıstanlı, H. A. (2017). Application of fuzzy AHP and VIKOR methods for supplier selection in an interconnect company. *Journal of Yasar University*, *12*, 40-54.

Snyder, L. V. (2006). Facility location under uncertainty: a review. *IIE Transactions*, *38*(7), 547-564.

Sundarakani, B., Pereira, V., & Ishizaka, A. (2021). Robust facility location decisions for resilient sustainable supply chain performance in the

face of disruptions. *The International Journal of Logistics Management*, *32*(2), 357-385.

Şengün, M. T., Siler, M., & Engin, F. (2018). Use of GIS in the selection of solid waste warehouse areas: sample of Malatya. *Zeitschrift für die Welt der Türken/Journal of World of Turks*, *10*(1), 159-180.

Şişman, B. (2017). Risk evaluating by fuzzy AHP and fuzzy VIKOR methods in failure mode and effects analysis for automotive sector. *Mehmet Akif Ersoy Üniversitesi Sosyal Bilimler Enstitüsü Dergisi*, *9*(18), 234-250.

Thanh, P. N., Bostel, N., & Péton, O. (2008). A dynamic model for facility location in the design of complex supply chains. *International Journal of Production Economics*, *113*(2), 678-693.

Wang, C.-N., Nguyen, N.-A.-T., Dang, T.-T., & Lu, C.-M. (2021). A compromised decision-making approach to third-party logistics selection in sustainable supply chain using fuzzy AHP and fuzzy VIKOR methods. *Mathematics*, *9*(8), 886.

Yeşilkaya, M. (2018). Selection of paper factory location using multi-criteria decision making methods. *Çukurova University Journal of the Faculty of Engineering and Architecture*, *33*(4), 31-44.

CHAPTER 2

HYDROGEOCHEMISTRY OF THE DRINKING WATER SOURCES OF THE BÜYÜKKIZILCIK REGION (KAHRAMANMARAŞ, TURKEY)

Prof.Dr. Yusuf URAS[1*], MSc. Volkan DALYAN[1], Prof.Dr. Yağmur UYSAL[2], Dr. Cihan YALÇIN[3]

[1] Kahramanmaras Sutcu Imam University, Geological Engineering Department, Kahramanmaras, Turkey. uras74@gmail.com; ORCID: 0000-0001-5561-3275.***Corresponding Author**

[2] Mersin University, Environmental Engineering Department, 33343, Mersin-Turkey. yuysal@mersin.edu.tr; ORCID: 0000-0002-7217-8217

[3] Ministry of Industry and Technology, General Directorate of Industrial Zones, Ankara, Türkiye, cihan.yalcin@sanayi.gov.tr

INTRODUCTION

Water is everything for life, and life without water is unthinkable. Even though the fact that ¾ of the earth is covered with water gives the appearance of abundance of water in the world, the rate of drinkable water is only around 0.74%. According to the World Wildlife Fund (WWF) research, more than 97% of the water on earth consists of salt water that is not suitable for human use. The ratio of potable water to the total amount of water in the world is less than 3% and most of this clean water is located in the poles. Therefore, the amount of water that can be used by human beings is less than 1% of the total water in the world. Groundwater ceases to be pure H_2O during the hydrological cycle and move by adding the substances in the environments they pass through. The type and amount of these substances are under the influence of many independent factors. Properties of groundwater can change depending on climatic conditions and water potentials. Therefore, many hydrogeological features such as origin, age, feeding regions, relations between rocks can be determined by the results of environmental isotope contents of these water sources.

This study was carried out with the aim of investigating the water resources of Büyükkızılcık location in Kahramanmaraş in terms of hydrogeochemistry and isotope geochemistry. It was also aimed to examine these drinking water resources in terms of water quality parameters and to investigate the possible public health effects of these parameters on the people living in the region in terms of medical geology. Büyükkızılcık, which is a part of Göksun district of Kahramanmaraş province, is 121 km from Kahramanmaraş and 33 km from Göksun. The spring waters of Büyükkızılcık region are provided from 5 sources called as Esen Village Watery Crack Spring (ECS-1), Büyükkızılcık Central Mosque Spring (BMC-2), Büyükkızılcık Central Spring (BM-3), Büyükkızılcık Central Healing Water spring (AC-4), and Büyükkızılcık Center Village Fountain (BM-5) (Figure 1 and 2).

Figure 1 General view of the research region

1. MATERIAL AND METHODS

1.1. Sampling Locations and Geology of the Study Region

Water samples were collected in different months over a period of 1 year (dry and rainy seasons) with the aim to evaluate the geological and water quality aspects of the drinking water sources of Büyükkızılcık region in Kahramanmaraş. Water samples were taken from five different water sources called as Esen Village spring (ES-1), Büyükkızılcık central mosque (BMC-2), Büyükkızılcık Central Spring (BM-3), Büyükkızılcık Central healing water source (AC-4), Büyükkızılcık central village fountain (BM-5) located in Büyükkızılcık region (Figure 1). The investigated water resources are located on the Elbistan L37–D2 map on the 1/25.000 map, and it is 121 km from Kahramanmaraş and 33 km from Göksun district. There are Başüstü and Ağcaaçar villages of Afşin district in the east of Büyükkızılcık, which is the research region, Turkish Sevin, Ören Stream in the northeast, Kepez, Yazıköy in the southeast, Karaömer and Düğünyurdu villages in the south, Yeniyapan, Kanlıkavak, Kömür, Esenköy and Kavşut villages in the west. It rests on the border of Sarız district of Kayseri province in the north (Figure 3).

The study region (Büyükkızılcık, Kahramanmaraş) is in the Taurus Orogenic Belt (Beyazpirinç 2005). According to its geological features, Kahramanmaraş and its surroundings are classified as Orogenic Belt (Engizek, Binboğa, Misis-Andırın and Malatya belt), Border Fold Belt, Fold Belt and Foreland (Gül 2000). In general, rock assemblages representing the

continental crust of the Taurus belt and the oceanic crust of the Neotethys in between, which came together due to the closure of the Neotethys ocean between the Anatolian plate and the Arabian plate, crop out in the region. Büyükkızılcık (Kahramanmaraş) region is located in the Binboğa belt and different rock groups are observed together in this region (Figure 4a).

The basement of the region is represented by these basement metamorphic rocks consisting of Yoncayolu (Özgül 1981) and Çayderesi formations belonging to the Permian aged Keban-Malatya Unit (Yılmaz et al. 1993; Yılmaz et al. 1987; Yumun and Kılıç 2002). These Paleozoic aged units are also cut by the Paleozoic aged Havcılar Granites (Baydar 1989; Uras and Çalışkan 2014). The Yoncayolu formation is mainly composed of alternations of gneiss, amphibolite schist and calcschist and contains intercalations of marble, recrystallized limestone, phyllite, quartzite and metavolcanite with medium thickness foliation in places. The Çayderesi formation, on the other hand, mainly includes marble, manganese marble, microcrystalline less dolomitic marble and metacarbonate lithologies that can be distinguished as lenses between recrystallized limestone and schists. Havcılar granite, on the other hand, consists of monzonite, granite and acidic sills and presents a folded structure together with metamorphic rocks (Uras and Çalışkan 2014). This Paleozoic basement is covered with angular unconformity by the Seske formation, which is given an Upper Paleocene-Lower Eocene age by Yılmaz et al. (1987). The unit mainly consists of neritic limestone with interbedded conglomerate and sandstone. The rocks in this region are side by side with dip-slip fault sets in some regions (Figure 1). There are hot water outlets associated with these fault zones and carbonation in the country rocks in these zones forms the dominant alteration type (Uras and Çalışkan 2014). Uras et al. (2018) revealed that hydrothermal alteration types are commonly seen in fluorite mineralization associated with fault zones, carbonate-propylitic alteration develops, and silicification and sericitization develop in places.

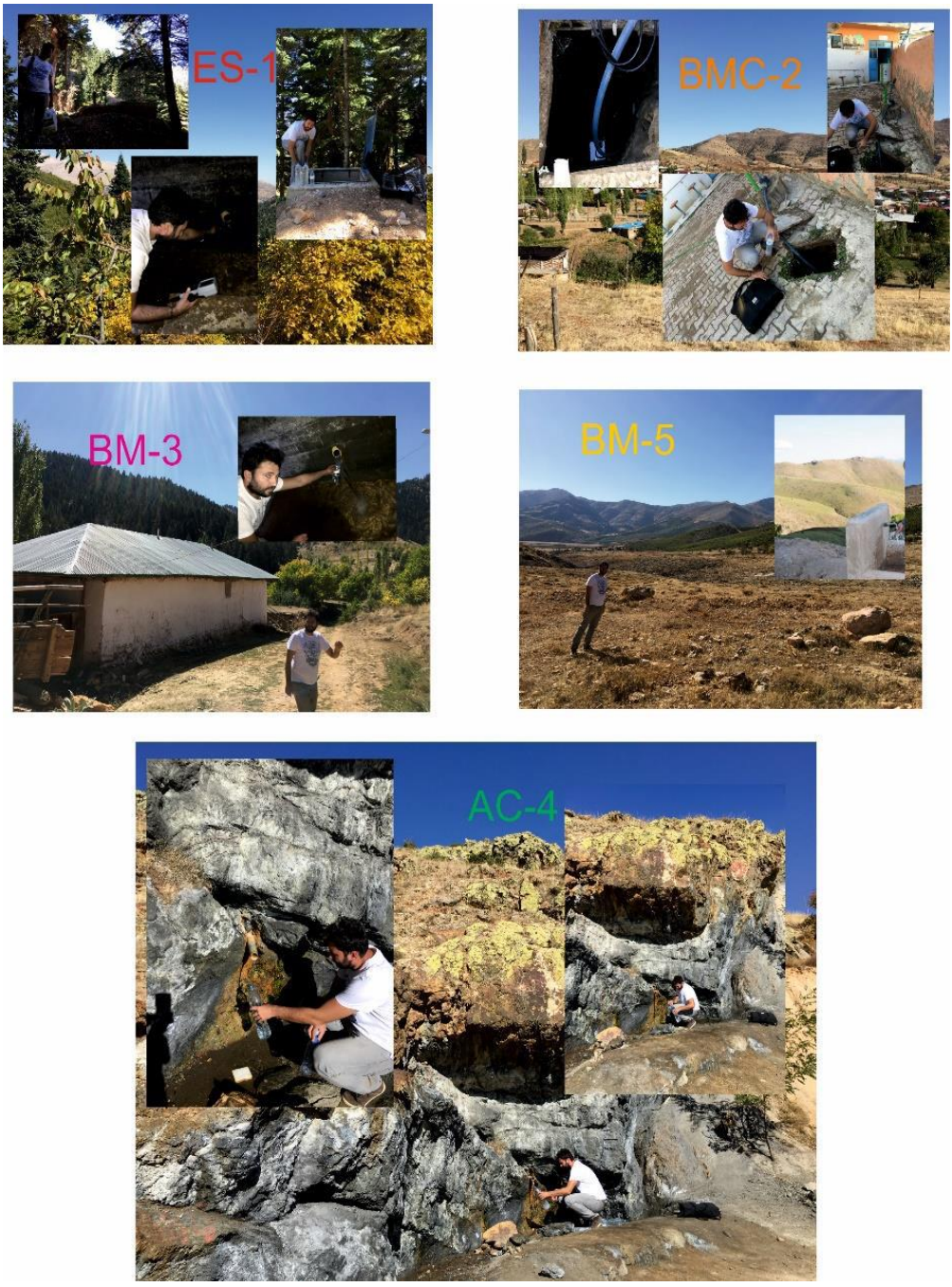

Figure 2 View of the Water Resources of Büyükkızılcık Region (ES-1, BMC-2, BM-3, AC-4, BM-5)

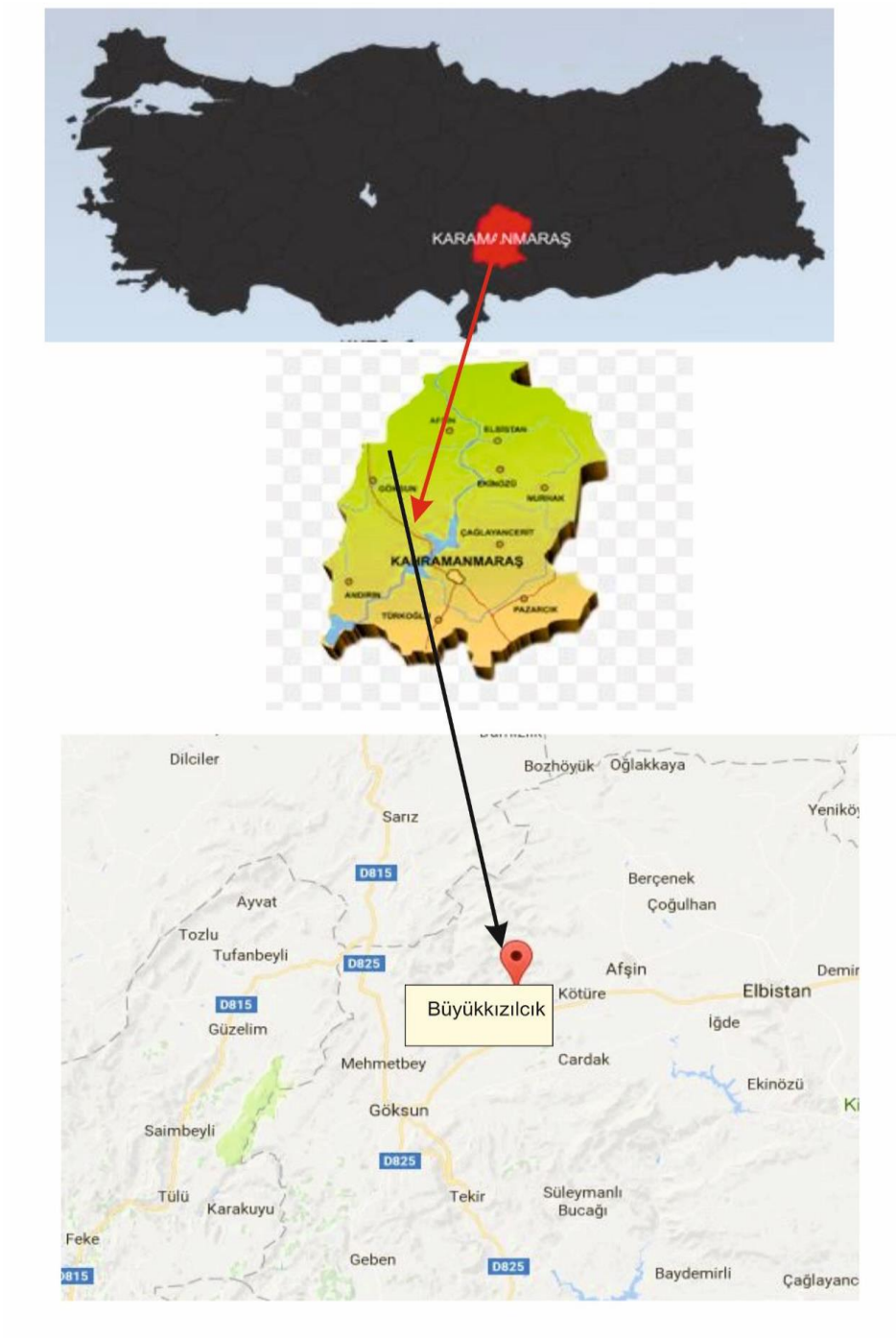

Figure 3 Location Map of the Investigated Region

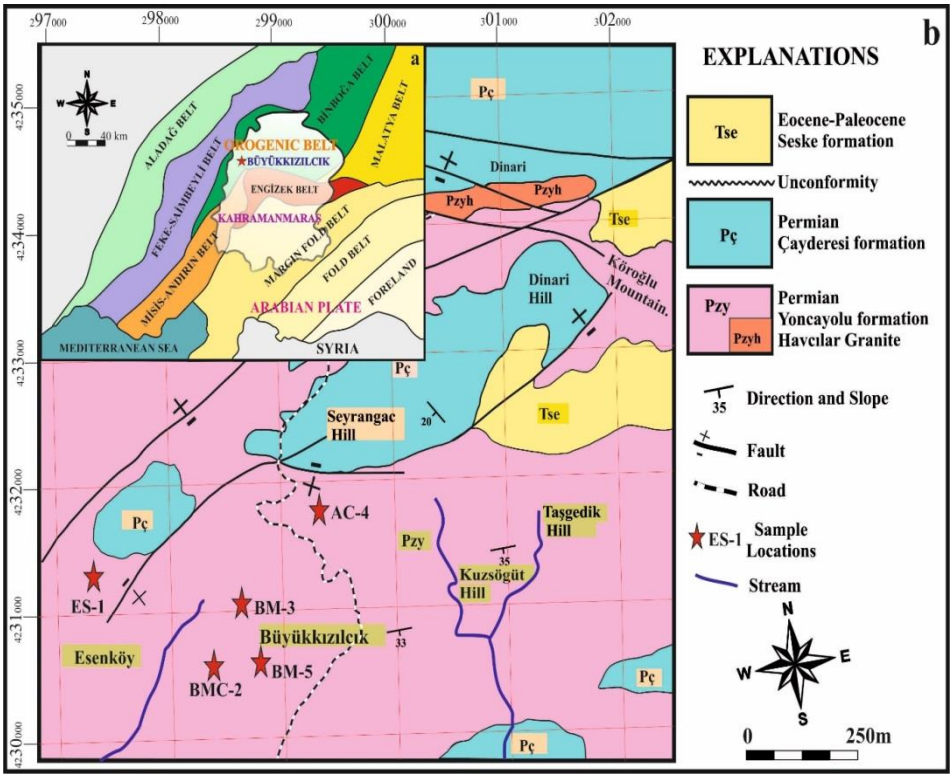

Figure 4 a) Tectonic Location of the Study Region According to Gül (2000), b) Geological Map of the Region (Ateş et al. modified from 2008)

1.2. Hydrogeology of Study Region

The Mediterranean Eastern Anatolia and Southeastern Anatolia areas of Turkey and the Kahramanmaraş Province are the nearest geographical neighbors, resulting in three distinct climate conditions in this area. Due to their higher elevation, the southern portions of Kahramanmaraş Province are thought to have a climate more akin to the "Degenerate Mediterranean Climate" than the northern parts of the province, which are thought to have a continental climate. Because of this, the research area has hot, dry summers while having warm, moist winters. The average amount of precipitation in the study region during the months of January through May and October through December exceeded 40 millimeters, according to long-term (1970–2012) monthly total precipitation records of the Turkish State Meteorological Service (TSMS 2017), but it did not exceed 10 millimeters during the months of June through September (Figure 5 and 6). However, the research area experienced significant precipitation (100 mm) from December through

February. As a result, it would seem that the region experiences consistent precipitation during the winter, spring, and fall seasons but not during the summer. However, according to data from the long-term (1970–2012) monthly maximum snow cover depth (TSMS 2017), the study region appears to have stayed covered with snow from December through March, with the deepest snow cover being attained in the month of February. Due to strong tectonic forces, the Yoncayolu formation, which is widely distributed throughout the study region and has a rich location in terms of surface waters because of the rainy and temperate climate characteristics mentioned above, exhibits a strongly jointed and fractured structure. Its structure makes the Yoncayolu formation porous in a way that permits surface waters to infiltrate deeper into the rock, where they can serve as an appropriate aquifer for storing deep infiltrating waters.

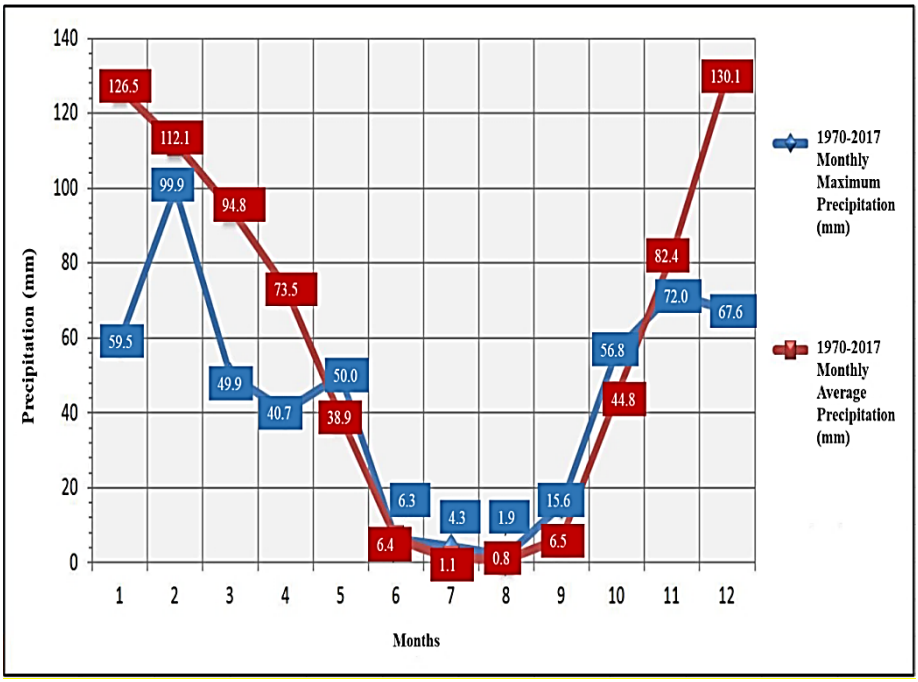

Figure 5 Change of Monthly Maximum and Total Precipitation Average for Many Years in Kahramanmaraş City Center and Its Vicinity, Including Büyükkızılcık Location (TSMS 2017)

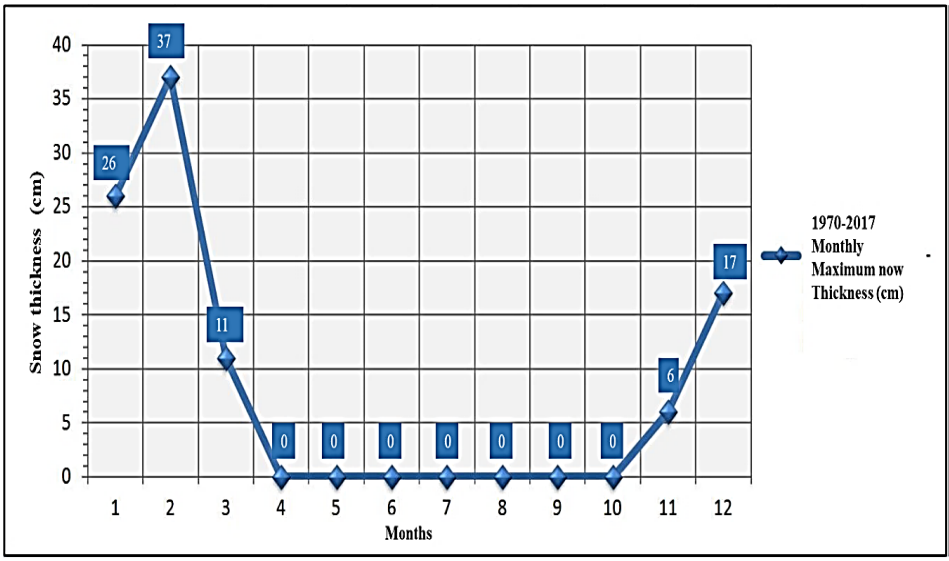

Figure 6 Change of Monthly Total Snow Thickness for Many Years in Kahramanmaraş City Center and Its Surroundings, Including Büyükkızılcık Location (TSMS 2017)

1.3. Methods

Five different water sources—Esen Village Spring (ES-1), Büyükkızılcık Central Mosque (BMC-2), Büyükkızılcık Central Spring (BM-3), Büyükkızılcık Central Healing Water Source (AC-4), and Büyükkızılcık Central Village Fountain (BM-5)—were sampled for water in order to assess the water quality of the drinking water sources in the study area. During sampling, a number of water properties were measured in situ, including temperature (Hanna HI 2211 pH/ORP), dissolved oxygen (DO), electrical conductivity (EC), and pH. Following that, the samples were transferred to the lab and kept there for additional tests in a refrigerator at 4 °C. Over the duration of a year, a total of 60 water samples were gathered from these five drinking water sources. The ACME Analytical Laboratories (Vancouver, BC, Canada) used ion chromatography (IC), inductively coupled plasma mass spectrometry (ICP-MS), and ICP-optical emission spectrometry (ICP-OES) techniques to analyze the heavy metal and anion-cation content of these samples. In the isotope laboratories of the Technical Research and Quality Control Department (TAKK) of the General Directorate of State Hydraulic Works in Ankara, Turkey, analyses of oxygen-18 (^{18}O), deuterium (^{2}H), and tritium (^{3}H) were performed (TRQC-Perkin Elmer QUAN-TULUS 1220).

According to established procedures (APHA/AWWA/WEF, 2017), water quality analyses were performed in triplicate for each analysis.

The water samples were initially categorized after the analyses on the drinking water sources of the Büyükkızılcık region, and the analytical results were compared against each other to establish a correlation between the samples and with other factors. The major goals of this chemical categorization were to identify the source of the waters, compare the concentrations of dominant and total dissolved ions, and establish whether the water from the various sources was safe for human consumption. As a result, we made an effort to analyze the heavy metal and anion-cation makeup of the groundwater samples and explain any anomalies in the measured data. The lithological characteristics of the rock units through which these waters flow are one of the key elements influencing the quality of water resources in the Büyükkızılcık region. As a result, it's crucial to determine the hydro-geochemical properties of the water sources and to pinpoint the lithological units that are in direct contact with them. The association between the hydrogeochemical properties of water resources and the hearing loss of the local population was also tried to be identified in order to expose the potential consequences of drinking water resources on human health.

2. RESULTS AND DISCUSSIONS

2.1. Hydrogeochemistry

In order to assess the quality of the drinking water sources in the Büyükkızılcık region, temperature, pH, EC, alkalinity, trace element concentrations, anion-cation composition, and metal concentrations measurements were made (Table 1). In addition to this, General Quality Criteria by Classes of Inland Water Resources were evaluated and shown in Table 2. Since the water resources in the Büyükkızılcık region range in temperature from 10 to 12°C, they are considered as cold waters. All water sources had similar DO% values (2.0-3.0%), however Na^+ concentrations varied from 2.21 to 14.61 ppm, which is substantially lower than the WHO's and WPCR's (Water Pollution Control Regulation) allowed limits of 200 mg/L and 125 mg/L, respectively. These low Na^+ concentrations indicate extremely low salt levels in these water sources. The water samples' low EC values (150–1300 µs/cm) further corroborate the idea that the water sources have extremely low ion concentrations and salinities. The ES-1, BMC-2, BM-3, and BM-5 spring waters have neutral or slightly basic characteristics, whereas the AC-4 source, which is a healing water source, has an acidic

character, according to an analysis of the pH values of Büyükkızılcık's water sources (pH: 3.23-3.92). Similar to this, Büyükkızılcık's water resources have extremely low heavy metal concentrations and are categorized as "very good" waters on the Wilcox diagram (Figure 7). According to the US Salinity Laboratory diagram, ES-1, BMC-2, BM-3, and AC-4 BM-5 sources are in the C_2-S_1 class, and BM-5 source is in the C_3-S_1 class (Figure 8). The findings of a chemical analysis were used to determine the hydro chemical characteristics of the waters in the research region. According to the Piper diagram, ES-1, BMC-2, BM-3, and BM-5 are waters containing $CaCO_3$ and $MgCO_3$ with a carbonate hardness of more than 50%, or carbonate hardness greater than non-carbonate hardness, and these waters are located in region 5 of the diagram (Piper, 1944) (Figure 9). This means that the non-carbonate hardness of the waters is more than 50% with permanent hardness, namely $CaSO_4$ and $MgSO_4$ waters. AC-4 is located in region 6. This means that the carbonate hardness is more than 50%. These waters are waters containing $CaSO_4$, $MgSO_4$, $CaCl_2$, $MgCl_2$. Anion–cation analyzes results of Büyükkızılcık water sources are shown in Table 3. The cation ranking of the water sources of ES-1, BM-3 and BM-5 was found as $Ca^{+2}>Mg^{+2}>Na^{+}+K^{+}$ while, found as $Ca^{+2}>Na^{+}+K^{+}>Mg^{+2}$ for the sources of BMC-2 and AC-4. The anion ranking of these samples was measured as $HCO_3^{-}>SO_4^{-2}>Cl^{-}$. As a result of the examination of water resources according to the Scholler diagram, it was seen that they were in the categories of “normal sulfate waters”, “normal chloride waters” and “hypo-carbonated waters” on the basis of sulfate, chlorine and carbonate-bicarbonate anion concentrations, respectively (Figure 10). According to the Turkish Water Pollution Control Regulation (WPCR, 2004) and the World Health Organization Drinking Water Standards (WHO 2017), these water resources examined in the Büyükkızılcık region are generally classified as Class I, while in terms of Mn and Cu parameters, they are Class II; It is classified as Class III for CI, DO (%), and EC parameters and as Class IV for DO (%), HM (excluding Mn, Al and Cu) parameters.

The Schoeller diagram is the diagram that gives the carbonate and sulfate saturations on the semi-logarithmic diagram (Schoeller, 1967) With the help of the Schoeller diagram, it is possible to get an idea about the origin of the waters and the formations they come into contact with. Schoeller classifies waters according to chloride, sulfate, carbonate amounts, ion-base exchange and anion-cation concentration relations. Chloride concentration is more important than others. This method, in which main anions and cations

are used, is a method preferred by geoscientists. The reason is that these diagrams provide an approach to determine whether the studied waters are of cognate origin and what type of formations they are in contact with. The anion-cation sequences determined in the water samples in the examined region are given in Table 1. According to the Scholler diagram, the drinking water sources in Büyükkızılcık may be divided into three categories based on their chloride, sulfate, and carbonate-bicarbonate concentrations: "normal chloride waters," "normal sulfate waters," and "hypo carbonated waters" (Figure 10). In addition, it was revealed that ES-1, BMC-2, BM-3 and BM-5 water sources were fed from the same aquifer, while the AC-4 source was fed from a different aquifer.

Table 1 Geochemistry of the drinking water sources of Büyükkızılcık Region

Geochemical Parameters		Water Sources			
	ES-1	BMC-2	BM-3	AC-4	BM-5
Temperature (^{0}C)	10.84±0.99	11.15±0.39	10.15±0.12	9.80±0.82	10.38±0.26
pH	7.34±0.21	7.55±0.26	7.29±0.29	3.58±0.25	7.12±0.07
EC (µS/cm)	262.6±23.5	200.2±55.69	152.25±33.88	200.2±55.69	1305.75±39.94
DO (mg/L)	2.83±1.26	3.0±0.95	3.08±0.90	3.0±0.95	2.83±0.83
Na^+ (ppm)	2.70±0.85	13.15±1.87	2.21±0.52	13.15±1.87	14.61±0.71
K^+ (ppm)	0.65±0.17	26.55±5.34	2.28±0.22	26.55±5.34	2.52±0.25
Ca^{+2} (ppm)	81.51±8.25	75.11±1.21	64.54±4.62	21.42±3.53	140.50±30.36
Mg^{+2} (ppm)	5.33±0.25	8.52±0.20	5.48±0.28	8.52±0.20	35.27±0.90
Cl^- (ppm)	74.36±1.38	400.58±141.48	2.64±0.70	3.32±0.23	126.84±42.39
HCO_3^- (ppm)	285.16±71.29	390,67±87,37	21.91±2.10	390.67±87.37	442.17±72.18
SO_4^{-2} (ppm)	8.69±0.32	24.03±0.27	134.47±6.95	24.03±0.27	78.55±4.05
Fe^{+2} (ppb)	10±1.01	10±0.95	10±0.70	11±0.75	11±0.75
NO_3^- (ppm)	16.59±2.15	22.34±1.38	4.64±0.50	2.35±0.21	126.91±0.46
F^{-1} (ppb)	50.0±22	150.0±20	20.0±30	1790±120	60.0±20
Al (ppb)	4.00±0.15	3.00±0.12	6.00±0.18	3144±21.5	2.00±0.10
Au (ppb)	<0.05	<0.05	<0.05	<0.05	<0.05
As (ppb)	7.50±0.03	7.50±0.02	7.10±0.02	102.20±11.02	0.50±0.12
Ba (ppb)	12.45±1.15	380.25±15.22	340.23±11.8	400.12±20.5	480.56±12.36
Total Cr (ppb)	11.30±2.86	13.70±1.35	10.10±1.14	10.80±2.21	10.60±092

Cu (ppb)	0.40±0.86	0.90±0.92	0.40±0.51	3.50±0.99	0.10±0.08
Hg (ppb)	<0.10	<0.10	<0.10	<0.10	<0.10
Mn (ppb)	1.26±0.06	1.24±0.10	1.02±0.16	0.03±0.01	0.45±0.15
Ni (ppb)	6.60±1.13	6.60±0.86	6.20±1.09	6.20±1.33	6.20±1.41
Sn (ppb)	<0.05	<0.05	<0.05	<0.05	<0.05
Pb (ppb)	<0.3	<0.3	<0.3	75.6±3.50	<0.3
Pt (ppb)	*NA.	*NA.	*NA.	*NA.	*NA.
Ru (ppb)	*NA.	*NA.	*NA.	*NA.	*NA.
Zr (ppb)	*NA.	*NA.	*NA.	*NA.	*NA.

*EC Electrical conductivity, DO dissolved oxygen; *NA: This parameter was not assigned*

Table 2 the classification of water sources according to "General quality criteria by classes of inland water resources"

Class of Water Quality	ES-1	BMC-2	BM-3	AC-4	BM-5
I	Temp., pH, EC, Na^+, Cl^-, SO_4^{-2}, Al	Temp., EC, Na^+, Al, SO_4^{-2}	Temp., EC, Na^+, Cl^-, Al, SO_4^{-2}	Temp., Mn, EC, Na^+, Cl^-, SO_4^{-2}	Temp., Mn, Na^+, Cl^-, SO_4^{-2}, Al
II	Mn,	Mn	Mn	Mn	Cu
III	-	DO	DO, Cl^-	DO	EC
IV	DO, HM (except Mn, Al)	DO, HM (except Mn, Al)	HM (except Mn, Al)	pH, DO, HM (except Mn)	DO, HM (except Mn, Cu, Al)

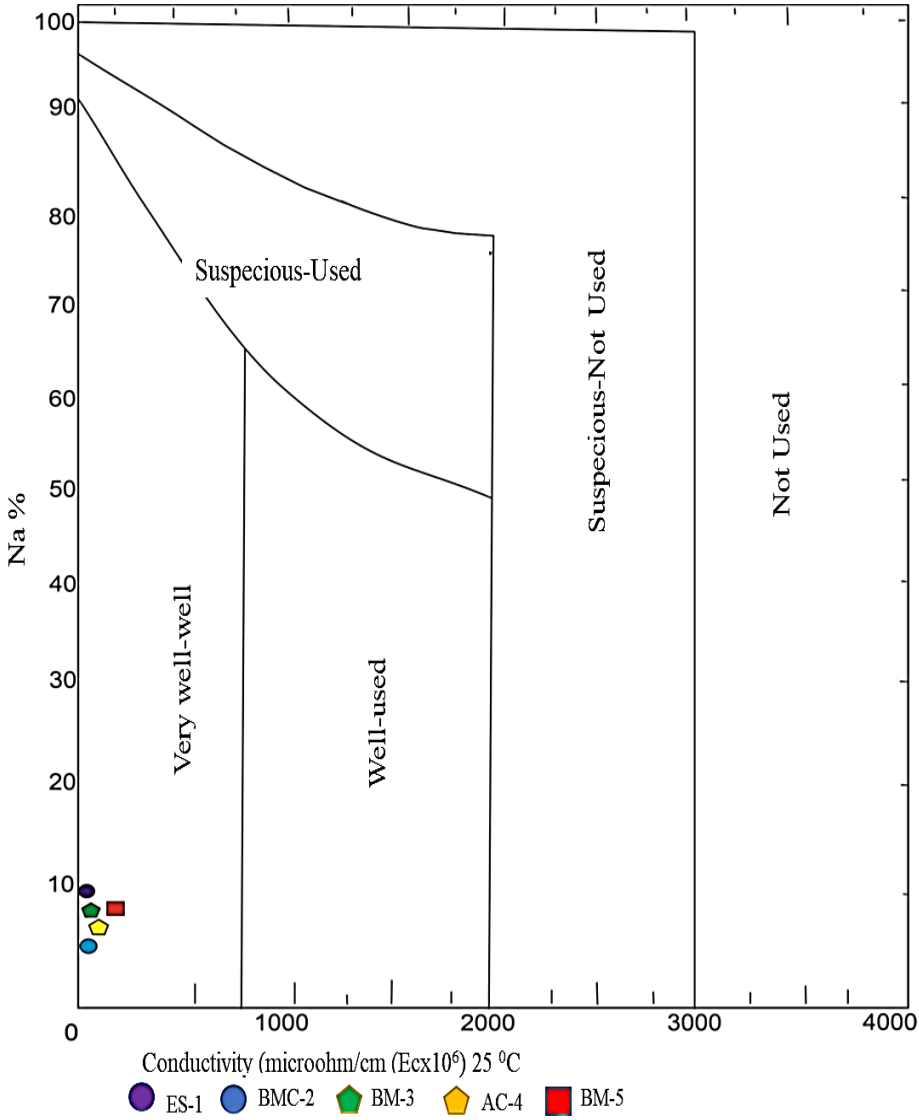

Figure 7 The Wilcox diagram of Büyükkızılcık drinking water sources

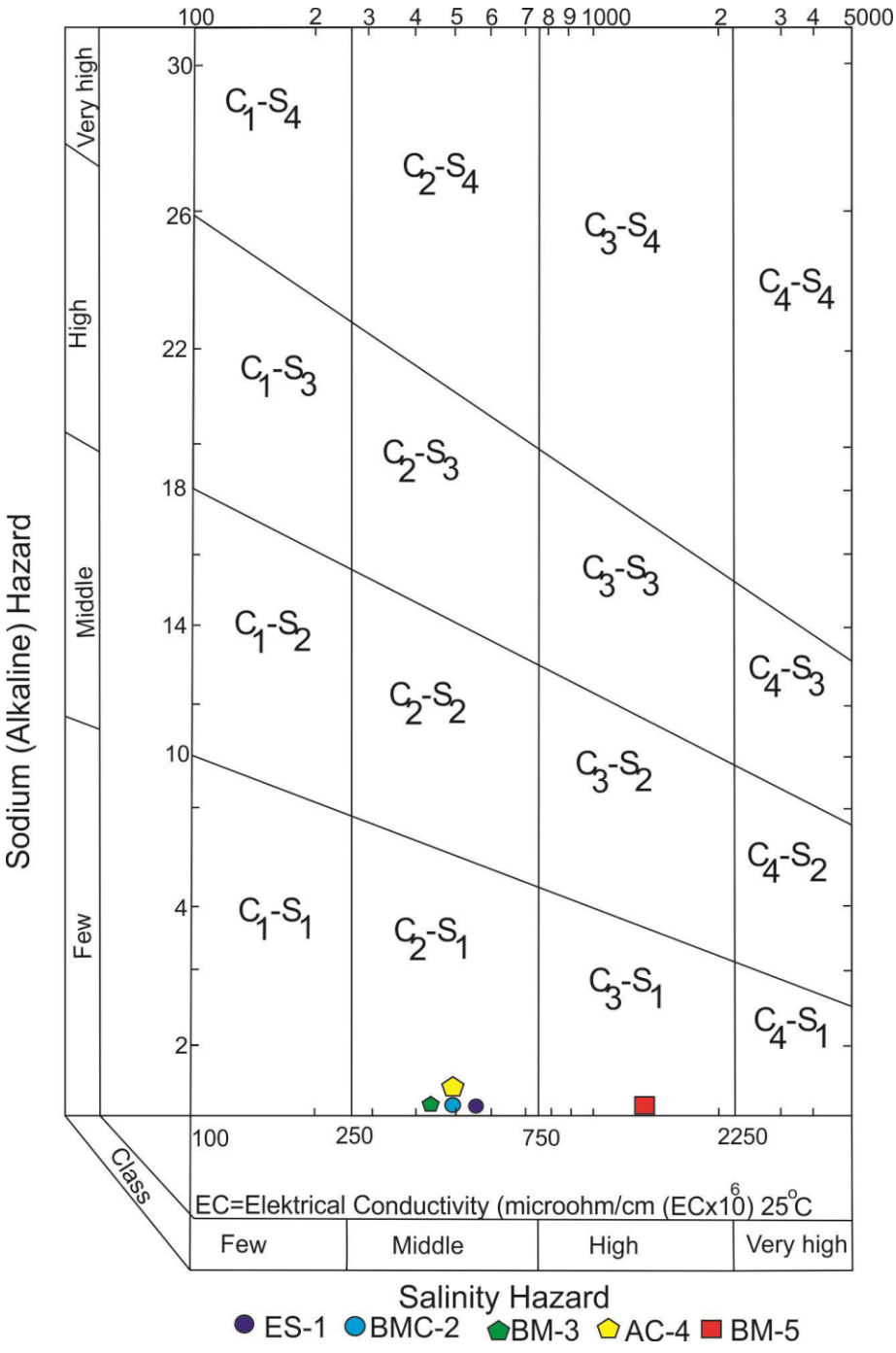

Figure 8 The U.S. Salinity Laboratory diagram of the drinking water sources of Büyükkızılcık

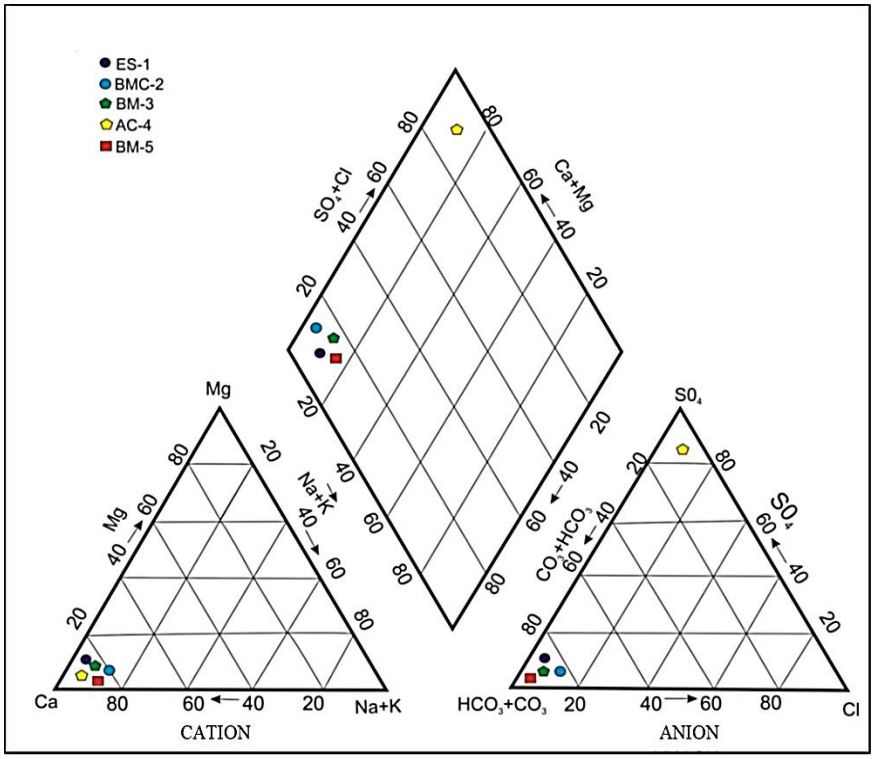

Figure 9 Piper diagram of the drinking water sources of Büyükkızılcık region. See Fig. 1 and footnote to Table 1 for explanations of the sampling sites/waters

Table 3 The anion–cation ranking of drinking water sources of Büyükkızılcık

Sample	Cation Ranking	Anion Ranking
ES-1	Ca>Mg>Na+K	HCO_3^->SO_4^{-2}>Cl^-
BMC-2	Ca>Na+K>Mg	HCO_3^->SO_4^{-2}>Cl^-
BM-3	Ca>Mg>Na+K	HCO_3^->SO_4^{-2}>Cl^-
AC-4	Ca>Na+K>Mg	HCO_3^->SO_4^{-2}>Cl^-
BM-5	Ca>Mg>Na+K	HCO_3^->SO_4^{-2}>Cl^-

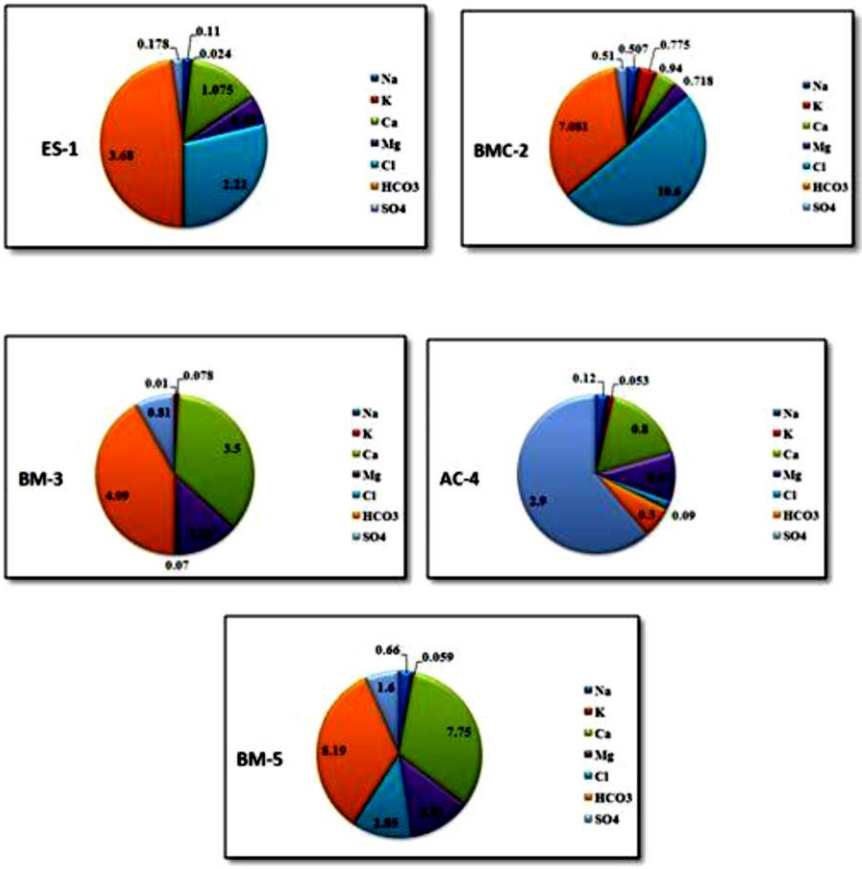

Figure 10 Pie diagram of water resources of Büyükkızılcık region

2.2. The results of isotopes

The researched subterranean water resources of Büyükkızılcık's aquifer characteristics and water-rock contact time were determined using environmental isotope measurements. Tritium (^{3}H), $\delta^{18}O$, and deuterium ($\delta^{2}H$) were used as radioisotopes and stable isotopes in these investigations, and the data were used to compute the recharge elevation values (Table 4). The results obtained were compared with the Global Meteoric Waterline (GMWL) and the Mediterranean Waterline (MWL) (Craig 1961). According to these values, it was determined that the water resources of Büyükkızılcık region are located between the global meteoric water line (GMWL) and the Mediterranean water line (MWL). Therefore, it has been concluded that the aquifers forming the water resources in the region are fed by meteoric precipitation and the

precipitation feeds the aquifer without evaporation. As a result of these interpretations, it can be said that the underground waters that feed the water resources are formed by the accumulation of precipitation under the ground by infiltrating along cracks, fractures and faults, and the stored groundwater reaches the earth by rising again along the faults and effective cracks. Deuterium excesses were calculated by using the formula of $d=\delta^2H - 8x\delta^{18}O$ (Dansgaard 1964).

Table 4 Results of the $\delta^{18}O$, δ^2H, and ^3H analyzes

Drinking water sources	Date (dry/rainy period)	Oxygen-18 δ^{18} O (‰)	Deuterium δ^2H (‰)	Excess value (d_e) (‰)	Tritium (^{3}H)
ES-1	August/April	-11.66/-10.86	-66.30/-67.24	26.30/19.64	3.72/3.51
BMC-2	Sept/April	-10.01/-11.11	-68.56/-65.42	23.84/23.46	4.53/3.42
BM-3	Sept/April	-11.46/-11.56	-70.01/-69.74	21.67/22.74	3.47/3.77
AC-4	Sept/April	-11.55/-11.59	-69.30/-67.44	23.01/25.88	3.55/3.82
BM-5	Sept/April	-10.99/-11.49	-68.04/-65.47	19.88/26.45	3.33/3.25

The Global Isotope Network (GNIP) is a value used to characterize the evolution of water throughout the hydrological cycle, with a global average of 10‰. The d-excess (>10‰) downwind of the eastern Mediterranean, which has a dry climate, is also generally high (Gat and Carmi 1970). High deuterium excess values indicate that marine precipitation is dominant, while low values indicate that these values are caused by terrestrial precipitation (Kehinde 1993). High deuterium excess points were observed in regions where marine rather than terrestrial precipitation are common. It was determined that the d_e range in the waters of Büyükkızılcık region was the lowest at 19.88 at BM-5 and the highest at 25.88 at AC-4. Table 4 showed

that d_e values of all water resources in the studied Büyükkızılcık region were above 10‰, and these water resources were under the influence of marine precipitation. By measuring the tritium content of water resources, it is aimed to determine the relative age and transition periods of these resources. According to the $\delta^{18}O$-Tritium graph, the spring waters of the Büyükkızılcık region are short-circulated waters of the same age, fed from low elevations (Figure 11a). In addition, BMC-2 spring water has a shallower circulation compared to other sources. In order to determine the residence time of the groundwater in the aquifer, the tritium values of the water resources were examined and it was found that the ^3H values in the water resources of the Büyükkızılcık location varied between 3.23-3.82. Considering that the waters, whose origin is meteoric, have low ^3H values due to radioactive decay as the circulation path extends underground, it can be said that the contact time of the spring waters of the Büyükkızılcık location with the aquifer is quite short compared to the low electrical conductivity values with high ^3H.

Tritium is one of the most important naturally or artificially radioactive tracers. The bleaching of tritium in precipitation is mainly from two sources. The first is the result of a natural event and is formed by the bombardment of nitrogen in the atmosphere by neutrons as a result of the effect of cosmic rays. The second source is artificial tritium, which has been released into the atmosphere as a result of thermonuclear experiments since 1952. Tritium values are generally used to find the age of waters in hydrogeology. Tritium-containing waters are generally young waters with transition periods of 5-10 years (Clark and Fritz 1997). The high ^3H and low Cl^- content of the water resources of Büyükkızılcık according to the Cl^--^3H graph showed that these water resources have aquifers fed by young groundwater (Figure 11b). According to the relationship between ^2H and ^3H, It was determined that the underground circulation time of the KS-2 source was longer than the other water sources (Figure 11c). A high ^3H value and a low EC value mean that the water-rock interaction of the water source is short-lived (<50 years' residence time) (Carreira et al. 2013). However, according to the Deuterium-Tritium relationship, it was determined that the circulation time of BM-5 source was slightly longer than other water sources (Figure 12d). It can be said that the above-mentioned isotope analysis interpretations and the general lithological characteristics of the Yoncayolu formation, which is located in the water resources of Büyükkızılcık location, are in great harmony. The Yoncayolu formation generally consists of

alternations of gneiss, amphibolite schist and calcschist. It also includes intercalations of medium thickness foliated marble, recrystallized limestone, phyllite, quartzite and metavolcanite. Due to the deformations it has undergone until today, the dolomite-dolomitic limestone, clayey limestone and quartzite levels in the unit, which has a highly fractured and fractured structure, have been reinforced with the effect of metamorphism and become more resistant to weathering with water. In addition, it can be said that even if the precipitations drain a little lower than the quartzite, it has gained a more resistant structure against weathering due to metamorphism and therefore cannot remain underground for a long time to dissolve the marbled dolomite-dolomitic limestone and clayey limestone lithology.

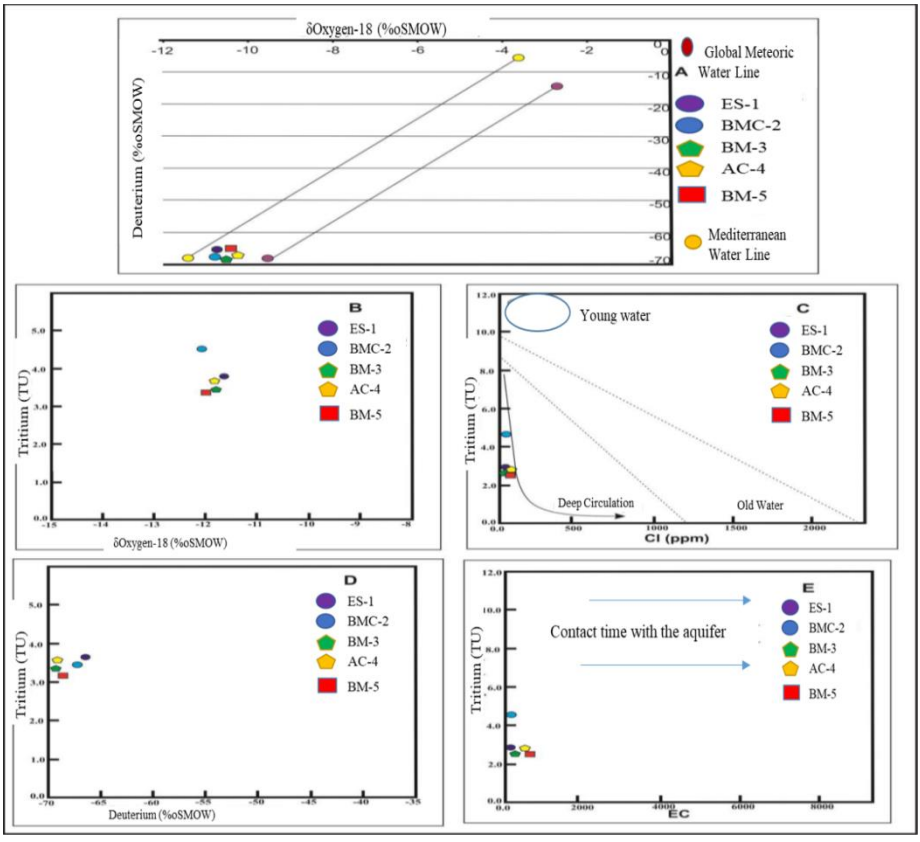

Figure 11 The Relationship Between Isotopes of Drinking Water Sources of Büyükkızılcık (**a)** $\delta^{18}O$-^{3}H; TU relationship, **b)** Cl-TU relationship, **c)** ($\delta^{2}H$)–TU relationship, **d)** (EC; µS/cm)–TU) relationship

2.3. Evaluation of water quality in terms of health

For human survival to continue, drinking-quality water is essential. Changes in water quality can result from both natural and artificial processes that occur in nature, some of which harm the water's quality. The hydrogeological properties of these water resources and, indirectly, the regional geological structure, have a considerable impact on the drinking water quality if the water is derived from groundwater and drunk without any treatment. Because of this, all across the world, water used for drinking reasons must meet a number of standards, regardless of its source. Since there is no wastewater mixing, drinking water sources, particularly in rural settlements, do not exhibit signs of industrial or anthropogenic pollution. These places also lack dense populations, urbanization, or industry. Because of this, groundwater is regarded as clean water and is typically consumed untreated. However, these streams will include different pollutants like heavy metals or arsenic if they have distinct properties because of the rock structure or if they are contaminated by different polluting sources like fertilizers, pesticides, or domestic wastewater. Metal ions are one of the most significant contaminants in water supplies due to their non-biodegradability, propensity for toxicity, and capacity to accumulate in the food chain (Githaiga et al. 2021). By drinking contaminated water, getting into contact with it on their skin, eating fish, or consuming crops that have been irrigated with it, humans can be exposed to metals in streams. Chronic health effects may result from the buildup of these chemical elements at low doses over time (Yuan et al., 2020). For instance, although cadmium is present in the environment in small levels naturally, it has been connected to cancer, hypertension, and anemia due to its increased presence in drinking water and other environmental factors (Karimi et al. 2020).

Pollutants in drinking and utility water can cause significant harm, especially to children. One of these pollutants is nitrate. Nitrates are a colorless, odorless and tasteless compound that can be found especially in well water and some groundwater. Nitrate can be represented chemically as NO_3^+ and NO_3-N (nitrate-nitrogen). According to US EPA criteria, its maximum level is 10 mg/l NO_3-N or 45 mg/L NO_3^+ (USEPA 2017). Compared to the standard values, the water source called BM-5 in the Büyükkızılcık region is above the normal drinking water standard values, especially in terms of nitrate. It was previously accepted that nitrate water values above this amount are harmful to babies and cause blue baby disease.

However, as a result of studies conducted in recent years, it has been concluded that it would be wrong to establish a direct link between nitrate in drinking water and the development of methemoglobinemia in infants, and that nitrate may be one of many factors that may be effective in the formation of this disease. The AC-4 water source, on the other hand, is above the drinking water standard values in terms of fluorine and sulfate parameters. Due to its significance in promoting the growth and development of human bones, fluoride in drinking water has also received a lot of attention (Xiao et al. 2022). When used sparingly, fluoride reduces tooth decay and strengthens bones. Over time, overly high fluoride intake can change how the body utilizes calcium and phosphorus, resulting in skeletal fluorosis and calcium insufficiency (Hu et al. 2021). The sources of fluoride in water include both natural processes (such as the interaction of water with rocks and fluoride-containing minerals) and human activities (such as the production of glass and ceramics, the use of phosphate fertilizer on agricultural land, and coal burning) (Ather et al. 2022). As a result of the rapid serious degradation of water resources and the associated risks to human health, there is an increasing need for enhanced attention to the quality of drinking water. Water quality assessments and risk assessments for human health are crucial for the national use and protection of water resources as well as for human health (Luvhimbi et al. 2022).

Sulfate mixes with groundwater from gypsum and anhydrite. Sulfur compounds are important pollutants with problems such as taste, odor, toxicity and corrosion that they form as a result of various reactions. Since sodium sulfate and magnesium sulfate have a laxative effect in humans, they are limited to an upper limit of 250 mg/L. It was determined that the potassium level was high in the BMC-2 water source. High potassium levels cause various health problems and threaten health negatively. Potassium elevation manifests itself in the human body in the form of fatigue, heart rhythm disturbance and vomiting. Potassium, a mineral necessary for bodily functions, is effective in the transport of oxygen to the brain and the regulation of heart rhythm. People with potassium deficiency experience heart rhythm disorders, loss of appetite, a feeling of fatigue, irritability and skin deterioration.

In a separate study we conducted on the drinking water sources in Derebogazi Village, Kahramanmaraş City, we discovered that despite the water sources in the region meeting drinking water regulations, they contained

very low quantities of calcium and magnesium cations (Uras et al. 2015). We learned about the locals through interviews and observations that they were shorter than average and that osteoporosis was prevalent in particular among their fragile bones. Therefore, even if calcium and magnesium are not heavy metal ions or other pollutants, consuming the anions and cations found in water sources on a regular basis in excess or incomplete form may eventually result in a number of health issues.

CONCLUSIONS

In this study, the water quality of five different water sources (ES-1, BMC-2, BM-3, AC-4 and BM-5) used by the people living in Büyükkızılcık region (Kahramanmaraş) as drinking water sources were investigated. The lithology of the region revealed a cracked and permeable structure that allowed the circulation of water in and within the Permian aged Yoncayolu formation. As a result of the evaluation of the chemical analysis results of the water samples taken for one year to determine the chemical properties of the water resources in the Büyükkızılcık region, ES-1, BMC-2, BM-3, BM-5 spring waters have the same aquifer lithology and the same origin according to the Schoeller diagram, while AC-4 spring water is of different aquifer origin. According to chloride, sulphate and carbonate + bicarbonate concentrations, these waters were classified as "normal chlorinated, sulphated waters", and "hypo-carbonated waters", respectively. According to the Piper diagram, ES-1, BMC-2, BM-3 and BM-5 water sources were classified as carbonate hardness more than 50%, while AC-4 source was in the class of waters with $CaSO_4$ and $MgSO_4$. According to the Wilcox diagram, ES-1, BMC-2, BM-3 and AC-4 sources were found in the C2-S1 water class, according to the US Salinity Laboratory diagram, the BM-5 source was in the C3-S1 waters class. The ^{18}O-^{2}H graph showed that the aquifers of the water resources in the region are fed by meteoric precipitation. High ^{3}H concentration, low EC values show that the groundwater of the region has short transit times with shallow circulation, and these water resources are in the young waters group with their age of < 50 years. According to the Cl-^{3}H graph, these waters are in the young waters group in terms of high ^{3}H and low Cl contents. According to the pH-EC values, the water resources of the Büyükkızılcık region are current waters with shallow circulation. According to the EC-^{3}H graph, the contact time of the water resources of Büyükkızılcık location with the aquifer is short. It has been observed that there is a great agreement between the isotope analyzes and the general lithological features

of the Yoncayolu formation, which is located in the water resources of Fatmalı-Önsen locality. It has been determined that the water sources of Yoncayolu locality water sources are in the very soft water class of the AC-4 water source, which offers an average of 20 mg/L $CaCO_3$ hardness value on an annual basis, in Kahramanmaraş and its surroundings, which generally have chalky and hard (10-50 FH) waters. Other sources are included in the general hard water characteristics of Kahramanmaraş city.

When evaluated in terms of medical geology, the AC-4 water source in the region was found to be above the normal drinking water standards, especially in terms of nitrate and sulfate parameters. It was seen that the waters in all regions were in compliance with the TSI 266, WHO and WPCR standards in terms of pH, temperature, electrical conductivity, sulfate, nitrate, ammonium and nitrite parameters, but the nitrate level was high in the Büyükkızılcık central village fountain (BM-5). There is a need for a study on nitrate removal in this source. Büyükkızılcık Central healing water spring (AC-4) was above the normal drinking water standards in terms of fluorine and sulfate. The high level of potassium in the source of the Büyükkızılcık central mosque (BMC-2) may cause various health problems and threaten health negatively.

REFERENCES

APHA/AWWA/WEF (2017) Standard Methods for the Examination of Water and Wastewater. 23rd Edition, American Public Health Association, American Water Works Association, Water Environment Federation, Denver.

Ates, S., Osmançelebioğlu, R. Özata, A., Karakaya, F.G., Aksoy, A.G., Mutlu, T.Y., Duman, O., Özerk, C., Yeleser, L., and Çiçek, İ. (2008). Kahramanmaraş İli ve Kentsel Alanların (İl-İlçe Merkezleri) Yerbilim Verileri, Ankara.

Ather D., Muhammad S., Ali W. (2022). Fluoride and nitrate contaminations of groundwater and potential health risks assessment in the Khyber district, North-Western Pakistan. International Journal of Environmental Analytical Chemistry, 1-16. https://doi.org/10.1080/03067319.2022.2098475

Baydar, O. (1989). Berit-Kandil dağları (Kahramanmaraş) ve civarının jeolojisi: İ.Ü. Fen Bilimleri Enst., Doktora tezi. İstanbul, 248 s,

Beyazpirinç, M. (2005). Geology of Keypez-Nisanıt-Domuzdere-Kitiz (Afsin-Kahramanmaras). Master Thesis, Çukurova University, Adana.

Carreira, P.M., Marques, J.M., Nunes, D., Santos, F.A.M., Goncalves, R., Pina, A., Gomes, A.M. (2013). Isotopic and geochemical tracers in the evaluation of ground water residence time and salinization problems at Santiago Island, Cape Verde. Earth and Planetary Science, 7:113–117. https://doi.org/10.1016/j.proeps.2013.03.063

Clark, I., Fritz, P. (1997). Environmental isotopes in hydrogeology. CRC Press/Lewis Publishers, Baton Rouge.

Craig, H. (1961). Isotopic variations in meteoric water. Science, 133:1702–1703. https://doi.org/10.1126/science.133.3465.1702

Dansgaard, W. (1964). Stable isotopes in precipitation. Tellus, 16:(4), 436–468. https://doi.org/10.1111/j.2153-3490.1964.tb00181.x

Githaiga, K.B., Njuguna, S.M., Gituru, R.W., Yan, X. (2021). Water quality assessment, multivariate analysis and human health risks of heavy metals in eight major lakes in Kenya. J Environ Manage, 297:113410. https://doi.org/10.1016/j.jenvman.2021.113410

Gül, M. A. (2000). Kahramanmaraş Yöresinin Jeolojisi. Hacettepe Üniversitesi Fen Bilimleri Enstitüsü Doktora Tezi, 304.

Hu B., Song X., Lu Y., Liang S., Liu G. (2022). Fluoride enrichment mechanisms and related health risks of groundwater in the transition

zone of geomorphic units, northern China, Environmental Research, 212, Part D, 113588. https://doi.org/10.1016/j.envres.2022.113588

Karimi, A., Naghizadeh, A., Biglari, H., Peirovi, R., Ghasemi, A., Zarei, A. (2020). Assessment of human health risks and pollution index for heavy metals in farmlands irrigated by effluents of stabilization ponds. Environmental Science and Pollution Research, 1-11. https://doi.org/10.1007/s11356-020-07642-6.

Kehinde, M.O. (1993). Preliminary isotopic studies in the Bida basin, central Nigeria. Environmental Geology, 22: 212–217. https://doi.org/10.1007/BF00767406

Luvhimbi, N., Tshitangano, T.G., Mabunda, J.T., Olaniyi, F.C., Edokpayi, J.N. (2022). Water quality assessment and evaluation of human health risk of drinking water from source to point of use at Thulamela municipality, Limpopo Province. Sci Rep. 12(1),6059. https://10.1038/s41598-022-10092-4.

Özgül, N. (1981). Munzur dağlarının jeolojisi: MTA Rap.No: 6995 136 s. Ankara.

Piper, A.M. (1944). A graphic procedure in the geochemical interpretation of water analyses. Eos, Transactions American Geophysical Union, 25: 914-928. http://dx.doi.org/10.1029/TR025i006p00914

Schoeller, H. (1967). Geochemistry of groundwater. An international guide for research and practice. UNESCO, 1967, chap 15, pp 1-18.

TSI 266, Turkish Standards Institute (2015). Water-Water Intended for Human Consumption

Turkish State Meteorological Service (2017). Available at: www.dmi.gov.tr.

U.S. Environmental Protection Agency (EPA) (2017). Water Quality Standards Handbook: Chapter 3: Water Quality Criteria. EPA-823-B-17-001. EPA Office of Water, Office of Science and Technology, Washington, DC. Accessed November 2018. https://www.epa.gov/sites/production/files/2014-10/documents/handbook-chapter3.pdf

Uras Y., Caliskan V. (2014). Geochemical patterns of the Buyukkizilcik (Kahramanmaras) fluorite deposits. Geochem. Int., 52(12), 1087-1100. https://doi.org/10.1134/S0016702915010061

Uras, Y., Abdelnasser A., Yalçın, C. (2018). Alteration geochemistry of the Buyukkizilcik fluorite deposits at Kahramanmaras region, Turkey: Implications for mass change calculations, VIII. Geochemistry Symposium, Abstract books, p. 322-323, 02-06 May 2018, Manavgat,

Antalya, TURKEY.

Uras, Y., Uysal, Y., Arikan, T.A., Kop, A., Çalışkan, M. Hydrogeochemistry of the drinking water sources of Derebogazi Village (Kahramanmaras) and their effects on human health. Environ Geochem Health 37, 475–490 (2015). https://doi.org/10.1007/s10653-014-9659-7

Wilcox, L.V. (1955). Classification and use of irrigation water. US Department of Agriculture, Circular 969, Washington DC.

World Health Organization (2017). Guidelines for Drinking-Water Quality: Fourth Edition Incorporating the First Addendum, Geneva. https://www.ncbi.nlm.nih.gov/books/NBK442373

WPCR, (2004). Water Pollution and Control Regulations. Official Gazette 31.12.2004, No:25687.

Xiao, W., Lin, G., He, X., Yang, Z., Wang L. (2022) Interactions among heavy metal bioaccessibility, soil properties and microbial community in phyto-remediated soils nearby an abandoned realgar mine. Chemosphere 286:131638. https://doi.org/10.1016/j.chemosphere.2021.131638

Yılmaz, Y., Gürpınar, O., Kozlu, H., Gül, M.A, Yiğitbaş, E., Yıldırım, M., Genç, C., Keskin, M., (1987). Maraş kuzeyinin jeolojisi (Andırın, Berit, Engizek-Nurhak-Binboğaz Dağları), yapı ve jeolojik evrimi: 97 s. İ.Ü. Mühendislik Fak., Istanbul.

Yılmaz, Y., Yigitbas, E., Genc, S.C. (1993). Ophiolitic and metamorphic assemblages of Southeast Anatolia and their significance in the geological evolution of the orogenic belt. Tectonics, 12(5), 1280-1297. https://doi.org/10.1029/93TC00597

Yumun, Z.U., Kilic, A.M. (2002). Stratigraphy of the region between Kamandagı and Camdere villages (Göksun-K.maras). Cumhuriyet University Bull., Serie A-Earth Sciences, 19, 193-202.

CHAPTER 3

OVERVIEW OF SERVICE DISCOVERY USING CLUSTERING WITH MOBILE AGENTS*

Dr. Begümhan TURGUT[1*]

[1] Artvin Çoruh Üniversitesi.ORCID No: 0000-0002-7594-9128.bturgut@gmail.com

* Taken from the author's master's thesis.

INTRODUCTION

As the complexity of networks in distributed environments rapidly increases in terms of the number of nodes, their mobility, wireless capabilities, heterogeneity of the nodes and so forth, the need for communication between the nodes becomes of paramount importance. Having strong connectivity among different entities in a network is an important issue to make possible for each entity to find one another and form a communication link, which does not always refer to a physical link. Service Discovery (SD) is the mechanism used for spontaneous discovery and dynamic configuration of entities; the entities may be service providers or resource entities. This chapter mainly focuses on giving an over of the service discovery in distributed environments where mobile agents are deployed, by incorporating the concept of clustering into an existing naming system while satisfying certain system parameters such as time-sensitivity and depth of search. There has been a lot of research work done in this field. Some of the existing works are applicable to generic functionality, whereas some are application specific. For this reason, an example application is included which reflects the kind of environment the SD can be applied to.

We provide an overview of clustering as well the motivation behind it, along with specific system parameters being accommodated. An overview of the concept of pervasive computing is given since most of the applications have been adapting the ideologies of this area of research. As communication among entities forms an essential part of any application, it will be an impetus for research on this area. Later, a sample case is presented to show how this can be applicable to some more realistic situations which is followed by a brief overview on related applications that service discovery can be utilized for.

Concept of clustering

The entities, which here are mobile agents in each distributed environment, should be able to join and leave the network without registering and deregistering. Since characteristics of these networks in terms of the number of nodes, mobility of nodes, and heterogeneity of nodes keep changing; service discovery in such environments becomes even more complex.

Each entity can make a request to find another entity. This request can either specify a particular destination or give a complex search query based on

attributes, to find a desired destination if such an entity exists. It is important to note that the requester would most likely not have any knowledge of the destination node. Also, it does not need to be concerned about the requester entity to know whether the destination entity exists or what its location would be, at the time of the search. The requester only knows what it is looking for and nothing further. The system should be able to handle the updates on each entity according to the mobility.

After the request is made, the SD would try to search for a destination(s) that matches the attributes specified in the request, if in fact it exists in the system. Rather than searching the entire network, if these entities were grouped into clusters [1] according to their attributes then the probability of a valid search would be higher, since each cluster would know it's one-hop neighbor. In this concept, valid search does not necessarily mean returning a non-empty result query; rather it refers to returning a valid response to give a view of the real situation. For example, the desired node might be in the network but for some reason the SD might not find it and return an empty query. The goal is to make sure that the SD can find the destination if it is in the network somewhere, and to decrease the search time. When a search on a particular cluster returns an empty result, then the search would be forwarded to the next one-hop neighbor rather than arbitrarily looking around the network. Because the entities are put into clusters based on their attributes, neighboring clusters would contain other entities with similar (or same) attributes. This way, the search would be forwarded along the desired route in terms of matching the attributes. As expected, if a destination entity exists, then the search using the clusters would take less time than searching the entire network without any particular direction specified.

If the requester does not specify the depth of the search, the entire network could be searched proceeding from one cluster to another [1]. However, if this parameter is given a value as to limit the number of times the forwarding actually occurs, then only a given number of clusters would be searched. This is pertinent, because as the search gets forwarded to the next and the next cluster, the result query might consequently get away from the desired attributes in terms of similarity. If the requester is looking for an exact match, then this is not an issue. Moreover, if the entire network is searched based on similarity, then some node that is not even close to the desired node could be returned as a result, which is not the goal. However, if the requester

is willing to negotiate to get to an end-node, which is like the desired node, then the depth of the search certainly needs to be specified.

Distributed Environments using Mobile Agents

Mobile agents are software entities in a distributed environment that carry out some set of operations on behalf of their user(s) or other program(s) with some degree of interdependence or autonomy and realize a set of goals or tasks for which they are designed. There are notable advantages [2] that are associated with deploying mobile agents in a distributed environment. Some possible benefits are discussed:

Applications in distributed systems that deploy mobile agents transparently use the network resources and the local resources in an efficient manner. One of the most important advantages of using mobile agents in a distributed environment is the reduction in network traffic. This can be attributed to the fact that code occupies less space than the related data. Mobile agents process data at the data source, rather than fetching it remotely. Since mobile agents are transferred to the sources of data, this leads to less traffic generated as compared to the case if the entire data itself were transferred [2].

Mobile agents also facilitate asynchronous communication between the nodes in an autonomous fashion. Tasks can be delegated to the mobile agents and be performed even if the delegating node becomes inactive at a later stage. In cases of failures in the functioning of the distributed system, the mobile agents can also help in providing mechanisms for fault tolerance [2]. This is accomplished by making the mobile agents increase the availability of certain agent-based services that can cater to the detection and correction of the faults that may occur in the system.

Mobile agents, when used in a distributed system, need to reside on limited number of nodes (one usually) at a given instant of time. This is a better approach than the traditional static server based approach where duplication of functionality was a necessity. Since mobile agents include the functionality within them, the need for duplication is greatly reduced. Moreover, the CPU consumption is also lowered. This leads to more efficient resource consumption [2] of the distributed system.

Mobile agents provide good support for the mobile clients, since the mobile client can make an agent-request, possibly when disconnected, launch

the agent during a brief intermittent connection session, and then get disconnected again. The responses may be collected in an analogous manner [3].

Another benefit of employing mobile agents is the secure frameworks they provide for communication. Mobile agents usually carry the user credentials along while they travel in a distributed system, and these credentials can be authenticated on execution at every node of the system [4]. There exist several effective encryption schemes that have been particularly devised for agent-based communication.

Observably, the restricted network resources in a distributed system like limited bandwidth, error-prone communication channels, portable devices, mobile clients, and so forth, are economically utilized by making use of mobile agents.

What is Pervasive Computing

The idea of pervasive computing was put forth by Mark Weiser in 1991, who described it as ubiquitous computing [5]—an environment which contains computing and communication capabilities and is integrated with the users, to the point of being ever-present. Some important issues related to the idea of pervasive computing environments, which have been described in greater detail in [6], are discussed in this section.

The notion of omnipresence merged with invisibility of the computing power is the key idea behind this area of research. It is believed that the user should be unaware of the computing environment that itself should be capable enough to sense the demands of the user and respond to them in an appropriate fashion. This leads to the idea of using smart spaces [6], which can be embedded with computing infrastructure.

Another key idea is the ability of the pervasive computing environment to hide the effects of transition from one sub-environment to the other, from the mobile user. The diverse sub-environments can be built on top of different underlying models. The idea is to mask [6] these variations that may otherwise seriously affect the seamless functioning of the infrastructure.

Two important ideas are proactivity and transparency—which are interdependent and enhance the capacity of the environment to actively interact with the user. Proactivity refers to automatically regulating the behavior of the environment based on needs or intentions or tolerance of the

user. But proactive nature of an environment can be overbearing to the user in either of the two cases: when the user does not actually need the fine-tuning of the resources in specific circumstances and when the user needs the resources to be fine-tuned but the frequency of the proactive responses of the environment is too high. The solutions to the problems encountered in each of the two cases mentioned above are tracking the intentions, needs, and tolerance of the user and incorporating transparency in the environment. The key is to make the pervasive environment context-aware [6]. This means that it must have knowledge of the user's past behavior, and the proactive responses must be made based on this context of the user. This context can be made of attributes like the location, state, history, and behavioral patterns of the user.

There are, however, complicated security and privacy issues that may arise owing to the environments' knowledge about the users' contexts. The trust between the user and the environment must be mutual and both need to be mutually dependent to get the desired optimum results.

The hardware resources in such an environment have higher demands for processing power, portability, and battery capacity. The ideas of energy-aware adaptation [6] and the various QoS schemes need to be augmented further. New distributed software paradigms need to be devised and the existing ones need to be improved further to incorporate the idea of pervasiveness.

Pervasive computing, per se, is increasingly becoming an important area of research that will revolutionize the ways in which computing has been used. Human-computer interaction, distributed components-based software design, artificial intelligence, wearable computing, portable mobile wireless devices, embedded computing systems-these are some of the other areas of research that are playing a pivotal role in the development of pervasive environments. This concept is also becoming widely used in distributed system such as the ones mentioned in the previous section.

Sample Applications

There exist a multitude of applications that service discovery could be applied to, ranging from systems used in academia, business, e-commerce, health, military and so forth. Especially with the rapid demand of Internet-based applications such as real-time multimedia portable device usage, cell phones, PDAs, tablets, and laptops; the areas related to wireless and mobile

networks have received much research interest. The complexity of the problems also has increased. As the intricacies involved in wireless networks: mobility, heterogeneity, and complexity of queries used - keep on extending, it becomes harder to handle service discovery in such environments where spontaneous and dynamic service providing is the goal. Finding the services (or entities) in each system used to be just based on IP address, however more complex queries are being implemented to find specific entities in more complex environments.

Sample Case

There are many applications that SD can be applied to, one of which is cited here as an example to show how a specific real-life situation can be used in an application system that utilizes service discovery. We consider a Crisis Management System (CMS) which can be any generic system used for managing contingencies ranging from natural disasters to vehicle accidents. It is important to note that the applications, or cases can be different depending on many factors such as time, place, severity, scope, and so on; however, given the environment and the CMS system, SD should be able to be applied despite the specific requirements. Thus, the case discussed next can be considered a demo to show how the system should be able to function in a particular case.

There are various contingency situations that can occur frequently all over the world, each requiring some kind of crisis management. Since some of them are more costly both emotionally and financially, this highlights the importance of development of a system that would handle majority of these cases. There should be a consideration on giving weightage to a set of given parameters such as having less user interaction, more timely response, higher rate of success which could translate into certain parameters such as time-sensitivity for SD.

There are on an average forty-two thousand deaths per year, twenty thousand of them being on site of the incident and rest in hospitals due to the auto accidents. It is reported that two hundred and sixty thousands of these are critical, five hundred thousand are hospital cases and two million are disability cases [7]. Financial costs incurred are also huge as the numbers follow: hundred billion dollars economically and three hundred and twenty-five billion dollars on comprehensive costs [7]. The statistics show very clearly that auto accidents hold a large portion of the crisis cases. Any vehicle

accident would be quite damaging as it is seen from the numbers as well. For this reason, an example of a train accident is given as an example in this context.

When CMS monitors trains to detect a crash happening, the identification and locating of the crash victims in a timely fashion would be the main goal as it could be seen in any other crisis situation such as natural disasters. The time factor is very important in any kind of crisis because it would make a difference on how successful the recovery can be. This puts a constraint on SD as well, since finding an entity in a timely fashion becomes essential. Next step would be to pass along the specific information regarding the passengers. To do this, the entity would need to find another entity which most likely could be an ambulance considering the situation.

A device is assumed to have been installed inside the train, perhaps in certain parts such as the beginning of the train, few points in the middle and towards the end of it. The device is assumed to contain a cell phone, crash sensor, GPS receiver, cell phone modem, and digital signal processor [7]. Since a cell phone would create an agent to place a call to an emergency operator and this agent would give service advertisement specifying what it is and what provides to become an active member in the distributed environment. If this does not go through, then the agent will try to form a communication with any other external entity. At this point, the agent would make a request to send a message to some entity that it does not know the location of, or even the knowledge of existence of such external entity may be unknown. Since the time taken for a successful search is very important, if SD does not return a result for the given query in a specific maximum threshold value, then the request would be made to a different server.

Even after the ambulance arrives, there can be a further need for SD. For instance, the ambulance might be looking for the nearest hospital that has a certain emergency unit to handle a specific injury. If the result returned contains multiple entries, then the requester might make a choice based on more specific query such as finding a facility with vacancy. This might be more important than finding one that is nearby but cannot handle the number of victims being transported. This is exactly why SD is used to look for a specific entity given an increasing number of complex queries depending on the situation. The entity being sought might also be mobile, in which case the process of locating it may become more complex.

Incorporating the idea of adding more sensors in the train to detect certain details as to how many passengers are on board could be part of extensions to provide SD for more specific queries. It becomes imperative to find possible solutions to improve the success probability of finding the right service using the SD.

There are various research projects being currently done for similar applications, in both academia and industry. Some of these are more application specific then others however in the essence of the base models are along the same lines. Some previous works related to different research projects include “Oxygen” at MIT, [8] “Portolano” at University of Washington, [9] “PIMA” at IBM T.J. Watson, [10] “Ninja” at UC Berkeley, [11] and “Aura” [12] at Carnegie Mellon University.

CONCLUSION

Service discovery will be a very important and critical feature of the future ubiquitous and distributed computing [6] scenarios. Discovery is used to refer to the mechanism of entities (and not simply the discovery services) discovering other entities and being discovered by the other entities over a network. A discovery service may be employed for lookup purposes - on the contrary, most of the lookup services do not support discovery. At base, clients must find relevant services, including sufficient information to establish contact and obtain service. There have been attempts to build architectures for service discovery, to be employed in the ubiquitous or pervasive environments. Performing service discovery using clustering with mobile agents is estimated to become an important part of distributed environments where time-sensitivity of processing is an integral part of the requirements.

REFERENCES

C.R. Lin and M. Gerla, “Adaptive clustering for mobile wireless networks,” IEEE Journal on Selected Areas in Communications, 15, 7, 1997, 1265-1275.

A. Bieszczad, B. Pagurek and T. White, “Mobile Agents for Network Management,” IEEE Communications Surveys,Vol. 1 No. 1, 1998.

D. Chess, C. Harrison, and A. Kershenbaum, “Mobile Agents: Are they a Good Idea?,” IBM Research Report, 1995.

Mitsubishi Electric ITA, Mobile Agent Computing: A White Paper, 1998.

Weiser, M., ‘The Computer for the 21st century,” Scientific American, September 1991.

M. Satyanarayanan, “Pervasive Computing: Vision and Challenges,” IEEE Personal Communications, August 2001.

The Center for Transportation Injury Research, CenTIR, Buffalo, NY. URL: http://www.cubrc.org/centir/index.html

John V. Guttag, “Communicating chameleons,” Scientific American, July 1999.

Esler, M., Hightower, J., Anderson, T., and Borriello, G., “Next Century Challenges: Data-Centric Networking for Invisible Computing: The Portolano Project at the University of Washington,” Mobicom’ 99.

Guruduth Banavar, James Beck, Eugene Gluzberg, Jonathan Munson, Jeremy Sussman, and Deborra Zukowski, “Challenges: An Application Model for Pervasive Computing,” IBM T. J. Watson Research Center.

Steven D. Gribble, Eric A. Brewer, Joseph M. Hellerstein, and David Culler, “Scalable, Distributed Data Structures for Internet Service Construction,” Fourth Symposium on Operating Systems Design and Implementation, O SD I2000.

Wang, Z, and Garlan, D., ‘Task-Driven Computing,” Technical Report, CMUCS- 00-154, School of Computer Science, Carnegie Mellon University, May 2000.

CHAPTER 4

IMPLEMENTING LATE EXHAUST VALVE OPENING AND INTERNAL EXHAUST GAS RECIRCULATION TO IMPROVE DIESEL EXHAUST SYSTEM WARM UP IN AUTOMOTIVE & MARINE VEHICLES

Assist. Prof. Hasan Üstün BAŞARAN[1]

[1] Izmir Katip Celebi University, Faculty of Naval Architecture and Maritime, Naval Architecture and Marine Engineering Department, Izmir, TURKEY. hustun.basaran@ikcu.edu.tr, 0000-0002-1491-0465.

[*]A prior version of this work is presented in the 23rd Congress on Thermal Science and Technology with International Participation (ULIBTK 2021) on September 8-10, 2021 / Gaziantep, Turkey.

INTRODUCTION

At present, most of the on-road vehicles and sea vessels are driven via use of diesel engines thanks to high efficiency and reliable operation. Many analysts predict that diesel engines will still be widely utilized in highway and maritime transportation in the coming future [Santos et al. (2021)]. There is an undeniable rising trend in electric on-road vehicles, however, internal combustion engines are expected to achieve 50% brake thermal efficiency target in the near future and thus, will have a sound place for highway and sea transport [Conway et al. (2021)]. Despite that high efficiency goal, diesel engines are currently faced with some strict regulations on exhaust-out pollutant rates that engine producers try to overcome [Dieselnet, China standards (2023)]. Automotive vehicles in the US are forced to perform with almost zero tailpipe NOx and PM rates due to stringent EPA standards [Dieselnet, US standards (2023)]. It is vividly shown in Figure 1 that there is a certain tightening demand for heavy-duty (HD) vehicles to minimize NOx and PM rates for the past thirty years in the United States [Gerald Liu & Munnannur (2020)].

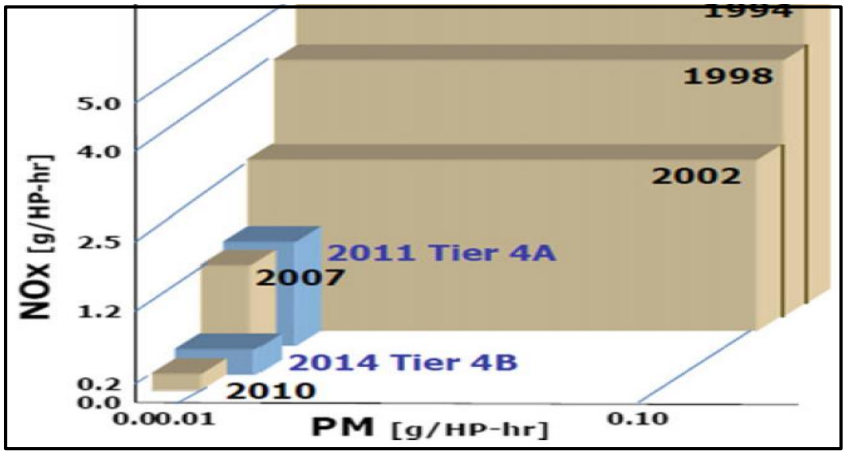

Figure 1: Progress of emission norms for HD diesel vehicles in the United States [Gerald Liu & Munnannur (2020)]

Considering those tightening emission norms in Figure 1, engine manufacturers are in an ongoing search to limit particularly NOx and PM rates [Fayyazbakhsh et al. (2022)]. One reliable and proven method applied by engine manufacturers is exhaust gas recirculation (EGR) [Wei et al. (2012)].

All exhaust gas is not discharged into the environment; some adjusted part of the flow is channeled back to engine cylinders to achieve low temperature, low oxygen medium and thus, low NOx rates in that strategy [Agarwal et al. (2011)]. In addition to EGR, some alternative fuels are widely used to reduce harmful pollutants in internal combustion engines [Noor et al. (2018)]. Diesel engines in ships are expected to decrease emission rates in the future via use of either liquefied natural gas (LNG), biodiesel, hydrogen or blended ratios of those with marine diesel fuel [Dos Santos et al. (2022)]. Those alternative fuels are also examined by researchers in modern on-road vehicles to meet stringent environmental regulations [Jeyaseelan et al. (2022), Zhang et al. (2022), Truong et al. (2021)]. Some recent innovative combustion techniques are considerably helpful to curb diesel emission rates as well [Krishnamoorthi et al. (2019), Singh et al. (2020), Pachiannan et al. (2019)]. Removing combustion-based engines and producing the driving power through high capacity batteries in vehicles is another rising trend to cut down on the emission rates [Hoekstra (2019), Andre et al. (2020)]. It is undeniable that electric or hybrid vehicles reduce harmful pollutants, however, they are also faced with some of the significant challenges such as high cost, incomplete infrastructure, heavy propulsion systems, long charging time and limited range, which need to be considered [Scrosati et al. (2015)]. Those disadvantages are not valid for current diesel or gasoline-fueled vehicles. Therefore, electric vehicles are not seen as a certain alternative for those vehicles at least in the near future.

The emission reduction potential of upper-techniques cannot be underestimated. In fact, EGR is one of the must-have methods for modern diesel engine systems to lower the NOx rates [Thangaraja & Kannan (2016)]. However, those strategies alone are unable to keep tailpipe emission rates below a certain level at all vehicle operation cases. Therefore, engine producers generally require exhaust after-treatment (EAT) systems in highway vehicles and ships to ensure sufficiently reduced emission rates [Xu et al. (2023)]. EAT systems are generally located very close to the turbocharger in an engine system. Those systems are built to filter the harmful pollutants at turbo-exit and then allow cleaned exhaust flow into the atmosphere. The whole EAT unit is normally made up of three basic sub-units as indicated in Figure 2: Diesel Oxidation Catalyst (DOC), Diesel Particulate Filter (DPF) and finally, Selective Catalytic Reduction (SCR), placed in sequence from the turbo-outlet to the atmosphere-outlet [Soleimani et al. (2018)].

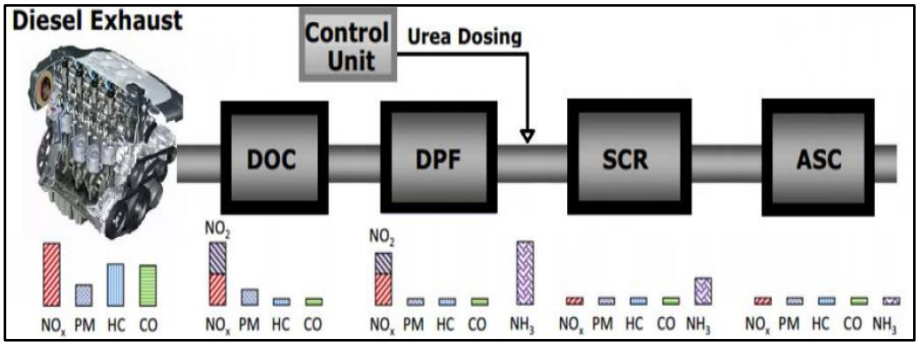

Figure 2: The layout of a modern automotive EAT system [Soleimani et al. (2018)]

Each subunit in Figure 2 has a distinctive aim to lower engine-out emission rates. DOC is mainly put in the system to control the unburned hydrocarbons (UHCs) and also carbon monoxide (CO) [Martinovic et al. (2021)]. DOC alone cannot deal with the PM rates. Therefore, DPF is used generally between DOC and SCR in EAT systems. DPF subunit is able to accumulate the soot particles via its particularly designed filter and then oxidize those particles through regeneration processes mostly before the PM overflows inside the unit [Zhang et al. (2023)]. Until the outlet of DPF, NOx is not thoroughly reduced in the EAT system. At this point, at DPF-exit, SCR is the paramount element to minimize the NOx rates. As demonstrated in Figure 2, there is a noticeable difference in NOx rates between the entrance and exit of SCR subunit. This is achieved through some complex chemical processes inside the system which requires the injection of some amount of ammonia (NH_3) on to the exhaust flow right before the inlet of the SCR subunit [Gabrielsson (2004)]. Ammonia slip catalyst (ASC) shown at the exit of SCR in Figure 2 is responsible to convert the leftover NH_3 into non-hazardous nitrogen and water [Jablonska & Palkovits (2016)].

Catalytic converters are highly effective to reduce undesirable emission rates of NOx, UHCs and PM. However, those devices cannot perform with their full potential at all highway or marine cruise conditions. For an effective filtering of harmful pollutants, their inner catalysts should mostly be maintained above 250^{o}C. As indicated on Figure 3 below, there is a sudden decline in NOx conversion efficiency of catalysts, particularly under 250^{o}C, in different SCR systems [Castagnola et al. (2011)]. Therefore, EAT systems at those low temperature conditions are unavailable to minimize emission rates satisfactorily [Vignesh & Ashok (2020), Feng et al. (2022), Wardana & Lim (2022)].

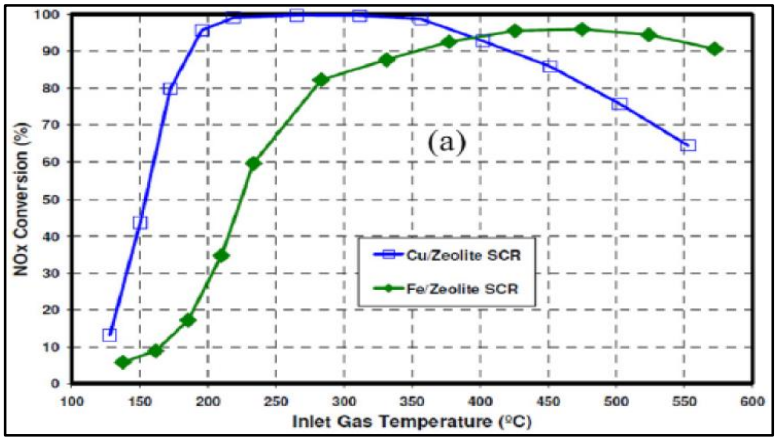

Figure 3: Change of NOx conversion efficiency of Cu and Fe SCR along inlet gas temperature [Castagnola et al. 2011]

EAT inlet temperature is normally determined in diesel vehicles via the hotness of exhaust temperatures. When the engine-out temperature is not sustained above 250°C, there is an unavoidable impairment in effectiveness of SCR systems, as shown explicitly in Figure 3. The problem with diesel vehicles is that they do not always work at high speeds which does not allow fuel-to-air ratio (FAR) to be kept at high levels. Therefore, at low-to-moderate speeds and loads, particularly during urban transport, FAR reduces to low levels and thus, causes cold exhaust temperature (below 250°C) and EAT systems with low conversion capacity. If the automotive vehicles are not equipped with a special warm-up device – a burner, a reformer, an electrical heater or a heat storage device – close to the engine system [Zavala et al. (2023), Jean & Goncalves (2023), Hamedi et al. (2019), Lee et al. (2014)], management of the exhaust thermal energy remains as the single measure to improve the diesel EAT units [Shuzhan et al. (2017), Basaran (2019), Wu et al. (2021)]. Control of engine valve timings is one of the recent and proven techniques to enhance thermal energy at EAT inlet [Joshi et al. (2022), Basaran & Ozsoysal (2017), Basaran (2020), Basaran (2021), Munnannur et al. (2022)]. Passivation of some of the cylinders is another reliable method for the same purpose [Hushion et al. (2022), Basaran (2018)]. In addition to cylinder deactivation, post-fuel injection is found to be rather useful to acquire high temperature at engine outlet in some recent works [Wang et al. (2022), Nie et al. (2022)]. There is also an attempt to apply multiple inner-engine methods to improve catalytic converter effectiveness [Guan et al. (2020), Basaran (2022)]. Those aforementioned efforts provide significant gains for after-treatment thermal management.

However, they mostly necessitate high fuel inefficiency [Honardar et al. (2011)]. Thus, the search for increased engine-out temperature via either inner-engine strategies or engine-independent methods such as electrical heating, after-burners or phase-change materials continues [Hu et al. (2023)]. The improvements achieved via those advanced methods can enable high-performance EAT and minimized NOx and PM rates in automotive and marine vessels.

This study intends to enhance diesel EAT unit heat up through simultaneous implementation of late exhaust valve opening (LEVO) and early exhaust valve closure (EEVC). Actuating valve timing is significant to control engine efficiency, undesirable losses, in-cylinder airflow and exhaust temperature at the entrance of the EAT unit. LEVO and EEVC are two reliable applications of that actuation which succeed to sustain exhaust temperature above 250^{o}C and thus, prevent the possible impairment of EAT operation. However, it is technically highly difficult to maintain multiple variable valve timing (VVT) operation in a real engine system which certainly needs to be considered by engine producers.

1. METHODOLOGY

In this study, an engine-dependent method is applied on a diesel engine model to increase the EAT-inlet temperature. VVT is generally technically difficult to apply on an automotive engine system. However, it is found to be noticeably useful to control exhaust temperatures in compression-ignition engines [Arnau et al. (2021)]. This analysis concentrates on the combination of two effective VVT cases: LEVO and EEVC. The implementation of those strategies is demonstrated in various Figures on the following subsections.

1.1. Engine Specifications and Model

Engine model specifications for diesel exhaust heat management are given in Table 1. Those kinds of engines are widely used in urban buses, shuttle vehicles or in relatively small sea vessels which have routes close to the shore. As mentioned earlier, those inner-city transport vehicles mostly face with low-speed, low-load navigations during urban traffic. The performance point in Table 1 can be considered as a low-loaded case for a heavy-duty vehicle. At 1200 RPM, with a relatively low load, 2.5 bar BMEP, temperature at EAT inlet remains at a cold level ($T_{exhaust}$ < 250^{o}C). That low-temperature medium mostly does not enable an effective filtering of the pollutants in the EAT system.

Table 1: Engine Specifications.

Model	Four-stroke heavy-duty diesel engine
Air intake	Turbocharged
Bore (mm)	107
Stroke (mm)	124
Compression ratio	17.3:0
Exhaust valve opening	20^{o}CA BBDC
Exhaust valve closure	20^{o}CA ATDC
Intake valve opening	20^{o}CA BTDC
Intake valve closure	25^{o}CA ABDC
Cylinder firing order	1-5-3-6-2-4
Calorific value of the fuel (kJ/kg)	42700
Operating speed and load	1200 RPM and 2.5 bar BMEP

The model of the engine system with properties used in the upper Table is indicated in Figure 4 [Lotus engine simulation (2020)]. The detailed layout of the model is presented in this plot. This analysis is achieved through using the model developed in former studies [Basaran & Ozsoysal (2017), Basaran (2020)]. Therefore, detailed mathematical analysis are given in those aforementioned references. In Ref. [Basaran (2020)], it is found that LEVO is a reasonable technique to boost EAT inlet temperature. However, the fuel penalty is so high (over 20%) that there is almost no room for practical application of LEVO. Therefore, in this follow-up work, the focus is to limit fuel penalty through combining LEVO with EEVC and achieve a practical method. Overall, proper exhaust valve lift modulation is addressed to reduce fuel consumption penalty.

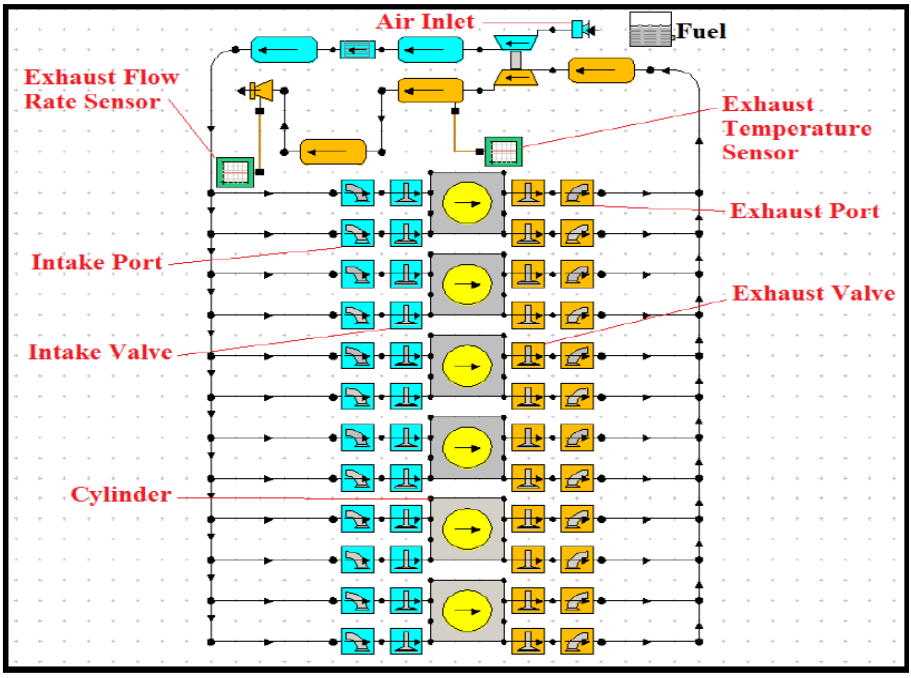

Figure 4: Detailed model of the diesel engine system

1.2. IEGR via EEVC Method

One reliable approach to elevate the gas temperature before the inlet of a catalytic converter system is to enable internal EGR (IEGR) in an engine system. Although there are some different methods such as negative valve overlap, exhaust valve reopening during intake stroke or exhaust valve phase shift to achieve this process, the easiest way is to modulate exhaust valve closure timing as shown in Figure 5. EEVC is maintained through advancing the exhaust closure alone in the system. Figure 5 points out explicitly that no other valve timing is actuated, all remain constant as EVC is swept through top dead center (TDC) and even beyond that. EEVC stops the exhaust discharge earlier than the nominal timing, 20^{o}CA after top dead center (ATDC), stated in Table 1 since it shortens the total opening duration of exhaust port in the system. Thus, some hot in-cylinder flow is not allowed to leave the system and mixed with the fresh flow of the next cycle. The analysis considers 8 consecutive steps seen in Table 2. EVC is moved backward until it is kept at 20^{o}CA before top dead center (BTDC).

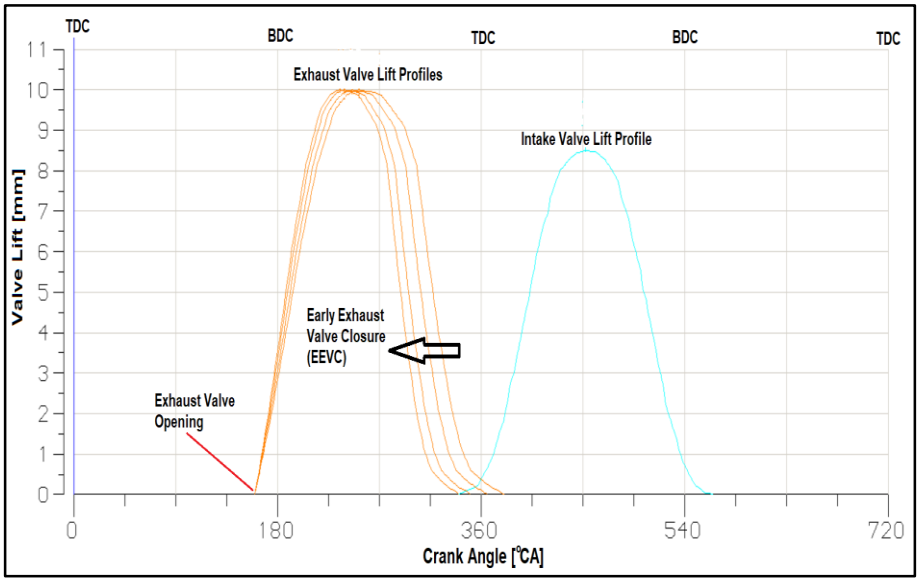

Figure 5: The application of EEVC method in the system

1.3. Combined LEVO+EEVC Method

In this section, LEVO and EEVC are coupled with the aim of boosting the EAT unit performance. While EEVC is the process of contracting the valve lift area from right to left, LEVO is the opposite. As vividly shown in Figure 6, LEVO tends to contract the opening duration from left to right. In other words, in LEVO mode, exhaust opening approaches TDC.

Unlike nominal mode, 20°CA before bottom dead center (BBDC) in Table 1, EVO in LEVO mode is far from the BDC and much closer to the end of the cycle. In LEVO+EEVC combined mode in Figure 6, intake valve lift form keeps its base condition. Similar to EEVC, LEVO has eight steps in Table 2 as this mode needs high EVO delay to attain exhaust temperature above 250°C. Unlike LEVO, LEVO+EEVC combined mode needs seven steps in Table 2 since this new mode requires lower EVO delay to achieve 250°C at EAT inlet.

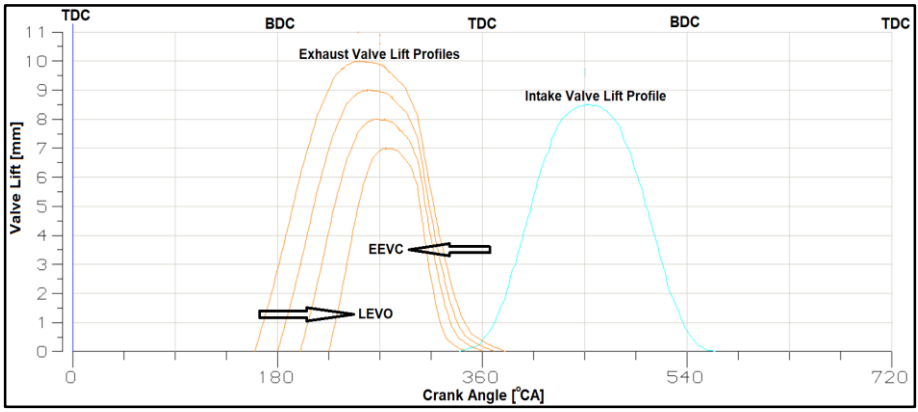

Figure 6: The application of Combined LEVO+EEVC in the system

Table 2: Main steps of different VVT methods.

Inner-engine Method	MAIN STEPS							
	1st	2nd	3rd	4th	5th	6th	7th	8th
EEVC (°CA ATDC)	15	10	5	0	-5	-10	-15	-20
LEVO (°CA ABDC)	7.5	-5	-17.5	-30	-42.5	-55	-65	-72.5
EEVC (°CA ATDC) + LEVO (°CA ABDC)	15 + 10	10 + 0	5 + -10	0 + -20	-5 + -30	-10 + -40	-15 + -45	

2. RESULTS AND DISCUSSION

The impact of LEVO, EEVC and LEVO+EEVC combined method on diesel performance is explicitly examined in this part of the work. The numerical analysis attempts to obtain the heat rise potential of the aforementioned modes on exhaust unit.

2.1. Effect of LEVO Timing on the System

LEVO is primarily investigated in this section with the goal of rising temperature around the inlet of the EAT unit. Figure 7 below shows the effect of LEVO on exhaust temperature and air-to-fuel ratio (AFR).

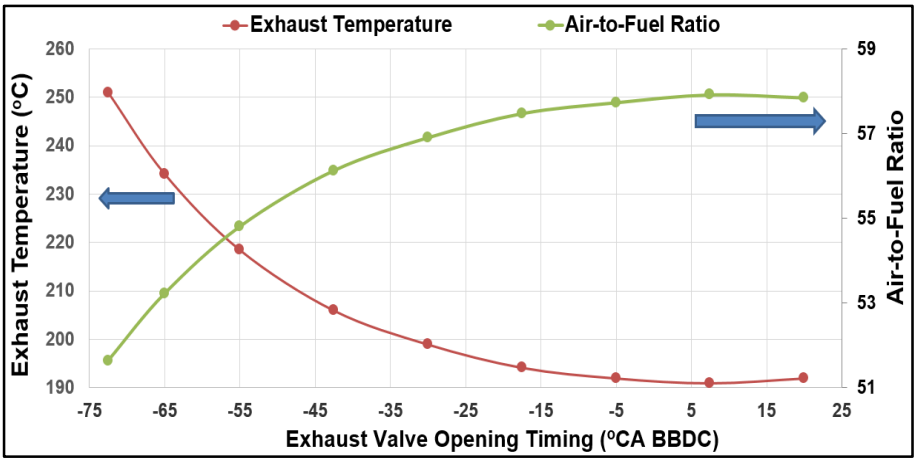

Figure 7: The impact of LEVO on exhaust temperature and AFR

As EVO is maintained further from the starting position, exhaust temperature is elevated consistently until its extreme mode of 72.5°CA ABDC. At low-retarded LEVO points, there is not a dramatic rise in temperature. However, at moderate and aggressive-retarded cases, the rise certainly speeds up. The LEVO mode succeeds to keep temperature over 250°C, however, it needs a noticeable delay of exhaust opening which is hard to control. As the temperature change is compared with AFR in Figure 7, it is seen that AFR has a definite role in detecting and controlling the engine-out temperature. It is demonstrated in several former studies that high exhaust temperatures require low AFR in diesel engine systems [Shuzhan et al. (2017), Hushion et al. (2022), Basaran & Ozsoysal (2017)]. Similar to those works, LEVO also results in a decline in AFR in Figure 7. Air-to-fuel ratio decreases from 58 at nominal mode to almost down to 51 at the highest delayed LEVO mode. AFR is normally altered via modulating either the airflow or fuel flow in a compression-ignition engine system. Change in airflow is mostly subject to actuation of intake valves which are fixed in LEVO mode. Thus, it is not considered as the primary reason why AFR goes down in Figure 7. Unlike airflow, fuel flow is closely related to exhaust valve design modifications. As illustrated in Figure 8, brake specific fuel consumption (BSFC) rises rapidly as exhaust valve continues to open in

later timings. Therefore, the main reason for low AFR in Figure 7 is due to the fuel penalty the system suffers in Figure 8.

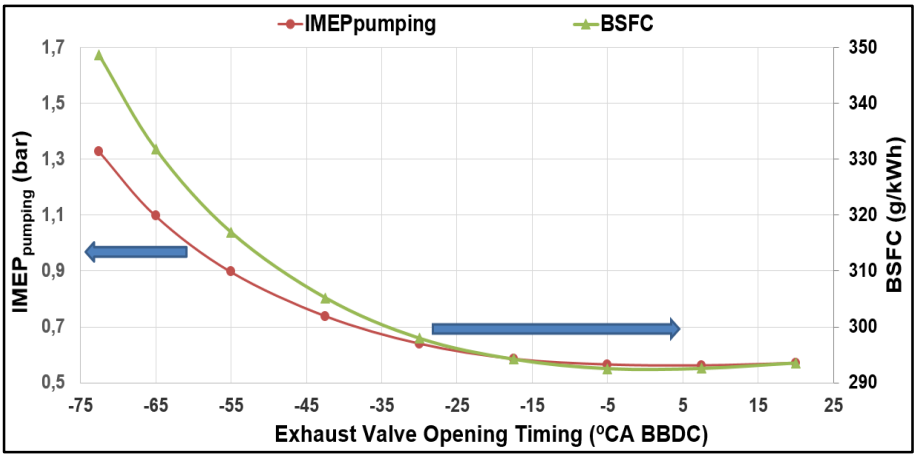

Figure 8: The impact of LEVO on pumping loss and fuel consumption

It is typically for diesel engines to have fuel penalty when especially the aim is to accelerate the exhaust heat [Honardar et al. (2011)]. In fact, exhaust heat is considered as the waste heat since it is one of the main terms of losses in both diesel and gasoline engines. Far from increasing the waste heat, it is often desirable to reduce it or at least reuse it to produce more work in highway vehicles [Hu et al. (2023)]. Similar to those previous works, LEVO leads to fuel inefficiency in Figure 8. That extra fuel requirement can be partially attributed to the increased pumping loss in the system. As EVO is delayed particularly further from the BDC, the piston starts to compress the in-cylinder gas, creating high in-cylinder pressure and thus, high $IMEP_{pumping}$ in the cycle. Overall, it can be derived that the stricter the LEVO is applied, the more substantial the pumping loss is and the greater the fuel energy required by the system to overcome the loss and keep engine load constant at 2.5 bar BMEP.

The unavoidable inefficiency incurred due to LEVO in the engine model can also be shown in Figure 9. Similar to Figure 8, thermal efficiency of the system goes through a serious reduction along the LEVO application. At baseline, the efficiency is maintained above 28%, whereas at the latest EVO timing it can barely pass 24%. Needless to say, that is a notable degradation and a serious drawback for LEVO.

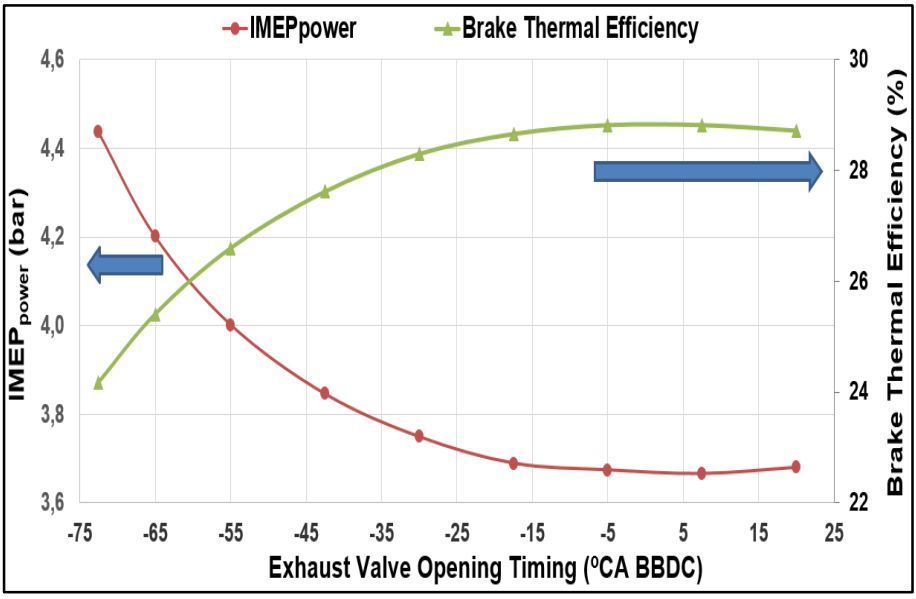

Figure 9: The impact of LEVO on $IMEP_{power}$ and brake thermal efficiency

Thermal efficiency worsens in Figure 9 since despite more fuel is utilized, engine load remains fixed. At constant speed, load can be regarded as the power capacity of the engine at hand. There is generally an anticipation to produce more power via higher fuel injection. However, as stated earlier, that excess fuel is used to offset the high pumping loss in Figure 8. Therefore, although the indicated power potential of the diesel engine – $IMEP_{power}$ – elevates in Figure 9, engine load does not rise. That additional energy partially compensates the extra loss due to $IMEP_{pumping}$ and also partially improves the exhaust temperature and heat as indicated in Figure 7.

Effect of LEVO on BSFC is critical. However, its effect on engine inlet & outlet flow rates is also crucial when an engine designer concentrates on the EAT heat-up process. Figure 10 displays the behavior of volumetric efficiency (η_{vol}) and exhaust flow rate as EVO is actuated in the model. LEVO seems to affect not only the temperature, as in Figure 7, but also flow rate of exhaust, as in Figure 10.

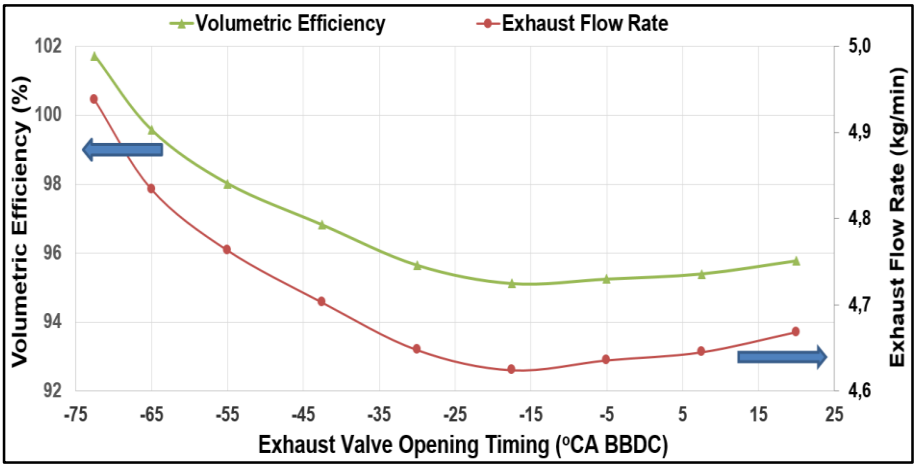

Figure 10: The impact of LEVO on volumetric efficiency and exhaust flow rate

The first impression from the plot above is that those two engine parameters go hand in hand. Whenever η_{vol} decreases, exhaust flow rate is reduced as well. As η_{vol} boosts, higher exhaust rate is observed in the model. The reason for low exhaust rates at slightly retarded EVO timings is that in-cylinder gas has shorter time to leave the cylinder and low engine-out flow causes lower expansion work in the turbocharger and thus, lower η_{vol} in Figure 10. On the other hand, as EVO is moderately or extremely delayed, exhaust rate climbs up due to the piston compressing the gas towards the TDC in the system. High exhaust rate leads to high turbocharger work and thus, high η_{vol} in Figure 10. Those increased η_{vol} and improved exhaust rates are favorable for rapid EAT warm up as the heat transfer from the outlet gas to DOC, DPF or SCR unit is conditional not only to temperature but also mass flow rate.

LEVO has a certain potential to yield optimum exhaust temperature and thus, high performance EAT units. However, it also owns a serious shortcoming – unacceptable inflation in fuel demand – as demonstrated in Figure 8 and Figure 9. As such, it is combined with EEVC in the following section to limit that high demand into acceptable levels.

2.2. Effect of Combined LEVO+EEVC on the System

LEVO-alone is found to be impractical in section 2.1. Thus, the co-application of LEVO and EEVC with the methodology mentioned in Figure 6 & Table 2 is proposed as a strategy with a low fuel penalty in this section. The impact of LEVO, EEVC and LEVO+EEVC combined techniques on BSFC and exhaust temperature is compared in Figure 11.

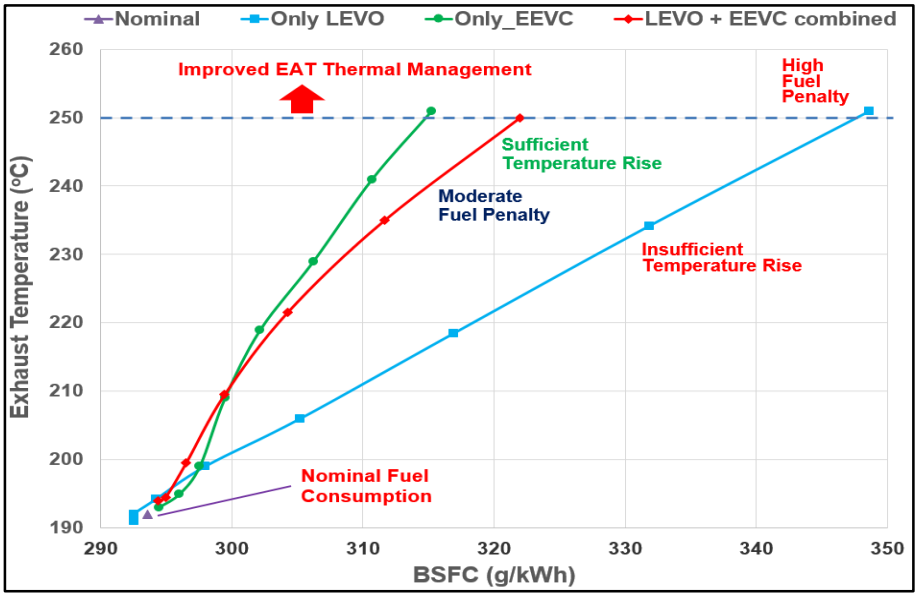

Figure 11: The potential of LEVO, EEVC and LEVO+EEVC combined methods on exhaust temperature rise considering the engine fuel penalty

The negative effect due to LEVO stands out among all methods in Figure 11. The fuel penalty the engine faces in LEVO-alone mode is much greater than that in EEVC-alone and LEVO+EEVC combined modes. Moderate use of LEVO in LEVO-alone mode is helpful to keep fuel penalty at a low level. However, in that case, the temperature rise is highly inadequate (much below 250ºC) to sustain effective after-treatment in diesel exhaust system. In contrast, EEVC-alone method requires the lowest fuel inefficiency in Figure 11. That stems from the fact that EEVC causes IEGR and decreases the engine η_{vol}, which denotes that there is lower mass to be heated inside the cylinders. That decreased in-cylinder mass is the advantage of EEVC mode for the fast temperature rise in Figure 11. As indicated earlier in Figure 10, LEVO is prone to raise the exhaust rate in the system. Unlike EEVC, that positive effect on mass flow rate is actually the reason why LEVO forces the engine system to consume the greatest amount of fuel to achieve 250ºC in Figure 11.

The LEVO+EEVC combined mode is different from both EEVC-alone and LEVO-alone modes in Figure 11. It is definitely advantageous compared to LEVO-alone method as it improves BSFC from as high as 350 g/kWh to almost 320 g/kWh. The reduced fuel penalty is obtained due to the use of IEGR in this mode. As shown in Figure 12, this moderate use of EEVC in combined

mode incurs relatively low exhaust rates which are not as evident as the ones calculated in EEVC-alone mode. This relatively diminished in-cylinder mass and also lower delay of EVO compared to LEVO-alone mode in Table 2 enable this new combined mode to realize the similar temperature boost in Figure 11.

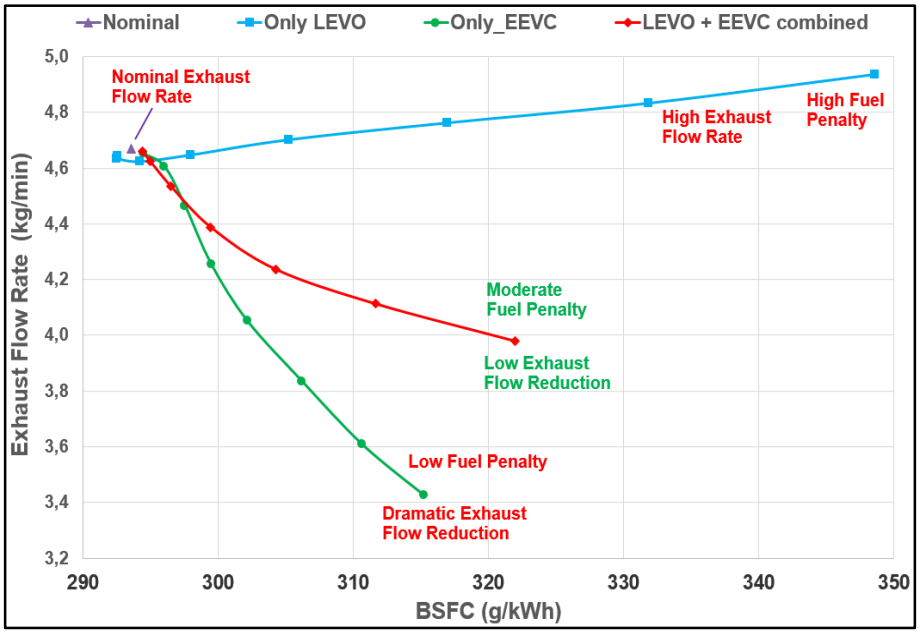

Figure 12: Change of exhaust flow rate in LEVO, EEVC and LEVO+EEVC combined methods considering the fuel penalty

LEVO-alone is seen to be the most beneficial for after-treatment warm up in Figure 12 as it enhances exhaust rates which none of other techniques is able to carry out in the analysis. However, high fuel penalty does not allow it as a viable option to implement steadily in diesel engine systems. EEVC-alone is so effective to enhance EAT inlet temperature. Nevertheless, it also brings about a substantial mass flow reduction which is likely to impair EAT heat up. The LEVO+EEVC combined method remains between those two extreme cases. It is capable of limiting the fuel penalty at an acceptable level, elevating the turbo-exit temperature above 250^{o}C and also it can avoid a possible deceleration in EAT heat up through maintaining the exhaust rates close to nominal mode which EEVC-alone mode fails to achieve.

2.3. Effect of Combined LEVO+EEVC on the EAT Unit

How single and multiple VVT methods influence engine-exit temperature and flow rates is discussed in the previous section. Now, using

those earlier calculations, it is possible to evaluate how each of those strategies actually is competent to speed up the EAT heat up operation. To determine the success of any method on EAT warm up, heat transfer rates to the catalytic converter need to be assessed. This assessment is achieved in the model utilizing the formula below [Incropera et al. (2007)]:

$$\dot{Q} = C\left[\dot{m}^{4/5}\right]\left[T_{exhaust} - T_{cataylst\ bed}\right] \quad (1)$$

The equation above is related to flow rate and temperature of exhaust, temperature of catalyst and a constant (C) specific to EAT unit used. The EAT warm up capacity of LEVO, EEVC and LEVO+EEVC combined methods is presented in Figure 13.

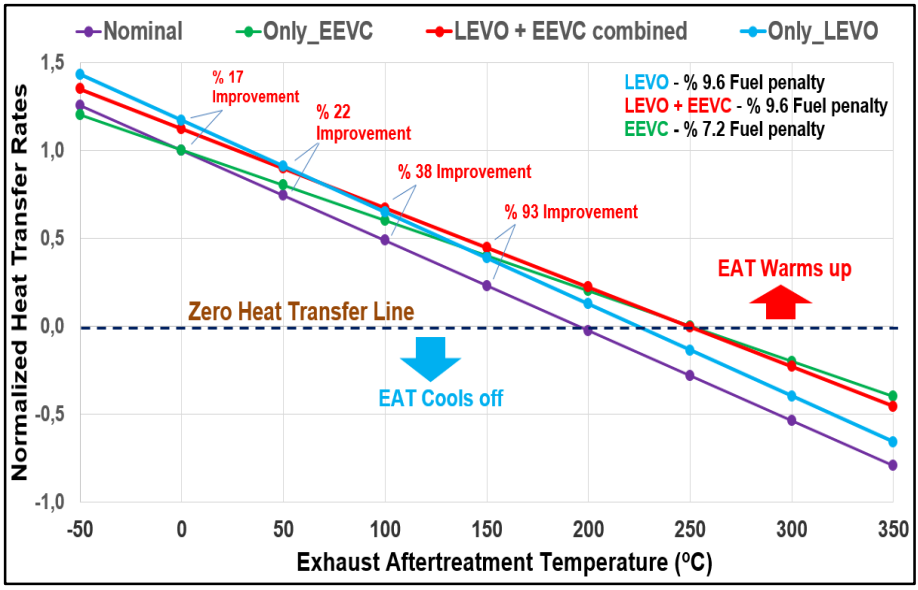

Figure 13: EAT heat up potential of LEVO, EEVC and LEVO+EEVC combined modes in comparison to the nominal mode

As fuel penalty is an important factor to be considered, the methods are applied in Figure 13 with the least fuel penalty each one causes while $T_{exhaust}$ surpasses 250ºC. EEVC-alone and LEVO+EEVC combined techniques can achieve 250ºC with 7.2% and 9.6% fuel penalties, respectively. LEVO-alone is limited to 9.6% fuel penalty and thus, it can only attain 220ºC in Figure 13. As the transfer rate in nominal mode at 0ºC is assumed as 1.0 (dividing by itself), all other transfer rates obtained via equation (1) is organized in accordance with this assumption (dividing each rate by the one calculated in nominal mode).

It is derived from Figure 13 that nominal mode is not consistent with effective thermal management. $T_{exhaust}$ is far below 250°C and thus, is unable to hold catalyst bed over 250°C. In contrast, EEVC-alone has the capacity to improve EAT above 250°C. However, it is only active after $T_{catalyst\ bed}$ exceeds 100°C since it distinctly lessens the exhaust rates, as in Figure 12. LEVO-alone is favorable at low catalyst temperatures (notably below 100°C) as it brings in extra exhaust rates, which none of other modes can carry out in Figure 12. Nonetheless, in this mode, EAT runs below 220°C although the system suffers up to 9.6% fuel penalty. Unlike LEVO-alone, LEVO + EEVC combined mode seems to be beneficial almost for all catalyst bed temperatures in Figure 13. This is attributed to improved transfer rates (up to 93%) due to accelerated temperature and controlled exhaust rates in Figure 11 and Figure 12, respectively. For the similar fuel penalty, LEVO + EEVC is superior to LEVO-alone not only during EAT warm up, but also during EAT cool off. Since this new mode has enhanced negative heat transfer rates (below zero transfer line) and thus, is able to delay a possible catalyst cool off much longer than other modes.

CONCLUSION

Current analysis attempts to investigate the impact of various VVT techniques on thermal maintenance of diesel after-treatment devices. Motivated from a previous work based on LEVO technique [Basaran (2020)], LEVO + EEVC combined method is performed in a diesel engine model to realize EAT warm up (T_{EAT} > 250°C) with improved engine fuel penalty. It is found that IEGR obtained through EEVC in LEVO + EEVC combined mode helps achieve EAT heat up in a fast, reliable and relatively decreased fuel penalty (from 20% to 9.6%) compared to both EEVC-alone and LEVO-alone modes. The proposed method is more effective not only at get-warm period (up to 93% more heat transfer rates), but also at stay-warm period of diesel EAT unit due to superior negative heat transfer rates.

REFERENCES

Agarwal, D., Singh, S. K., & Agarwal, A. K. (2011). Effect of Exhaust Gas Recirculation (EGR) on performance, emissions, deposits and durability of a constant speed compression ignition engine. Applied energy, Vol. 88(8), pp. 2900-2907.

Andre, M., Sartelet, K., Moukhtar, S., Andre, J. M., & Redaelli, M. (2020). Diesel, petrol or electric vehicles: What choices to improve urban air quality in the lle-de-France region? Atmospheric Environment, Vol. 241, p. 117752.

Arnau, F. J., Martin, J., Pla, B., & Aunon, A. (2021). Diesel engine optimization and exhaust thermal management by means of variable valve train strategies. International Journal of Engine Research, Vol. 22(4), pp. 1196-1213.

Basaran, H. U. & Ozsoysal, O. A. (2017). Effects of application of variable valve timing on the exhaust gas temperature improvement in a low-loaded diesel engine. Applied Thermal Engineering, Vol. 122, pp. 758-767.

Basaran, H. U. (2018). FUEL-SAVING EXHAUST AFTER-TREATMENT MANAGEMENT ON A SPARKIGNITION ENGINE SYSTEM VIA CYLINDER DEACTIVATION METHOD. Isı Bilimi ve Tekniği Dergisi, Vol. 38(2), pp. 87-98.

Basaran, H. U. (2019). Improving exhaust temperature management at low-loaded diesel engine operations via internal exhaust gas recirculation. Dokuz Eylül Üniversitesi Mühendislik Fakültesi Fen ve Mühendislik Dergisi, Vol. 21(61), pp. 125-135.

Basaran, H. U. (2020). Utilizing exhaust valve opening modulation for fast warm-up of exhaust after-treatment systems on highway diesel

vehicles. International Journal of Automotive Science and Technology, Vol. 4, No. 1, pp. 10-22.

Basaran, H. U. (2021). Effects of Intake Valve Lift Form Modulation on Exhaust Temperature and Fuel Economy of a Low-loaded Automotive Diesel Engine. International Journal of Automotive Science and Technology, Vol. 5, No. 2, pp. 85-98.

Basaran, H. U. (2022). Late Fuel Injection Combined with Retarded Intake Valve Closure for Improved Exhaust System Warm-up in Diesel Automotive Vehicles. Sustainability of Natural Resources' Efficiency, pp. 33-60.

Castagnola, M., Caserta, J., Chatterjee, S., Chen, H. Y., Conway, R., Fedeyko, J. (2011). Engine Performance of Cu- and Fe-Based SCR Emission Control Systems for Heavy Duty Diesel Applications. SAE Technical Paper, No. 2011-01-1329.

Conway, G., Joshi, A., Leach, F., Garcia, A. & Senecal, P. K. (2021). A review of current and future powertrain technologies and trends in 2020. Transportation Engineering, Vol. 5, 100080.

Dieselnet, China standards. http://www.dieselnet.com/standards/cn/hd.php#stds (Retrieved: 09.02.2023)

Dieselnet, US standards. http://www.dieselnet.com/standards/us/hd.php#stds (Retrieved: 09.02.2023)

Dos Santos, V. A., Pereira da Silva, P., & Serrano, L. M. V. (2022). The Maritime Sector and Its Problematic Decarbonization: A Systematic Review of the Contribution of Alternative Fuels. Energies, Vol. 15(10), No. 2, p. 3571

Fayyazbakhsh, A., Bell, M. L., Zhu, X., Mei, X., Koutny, M., Hajinajaf, N. & Zhang, Y. (2022). Engine emissions with air pollutants and greenhouse gases and their control technologies. Journal of Cleaner Production, Vol. 376, 134260.

Feng, S., Li, Z., Shen, B., Yuan, P., Ma, J., Wang, Z. & Kong, W. (2022). An overview of the deactivation mechanism and modification methods of the SCR catalysts for denitration from marine engine exhaust. Journal of Environmental Management, Vol. 317, 115457.

Gabrielsson, P. L. (2004). Urea-SCR in automotive applications. Topics in catalysis, Vol. 28, pp. 177-184.

Gerald Liu, Z. & Munnannur, A. (2020). Future Diesel Engines. Design and Development of Heavy Duty Diesel Engines: A Handbook, pp. 887-914.

Guan, W., Pedrozo, V. B., Zhao, H., Ban, Z. & Lin, T. (2020). Miller cycle combined with exhaust gas recirculation and post-fuel injection for emissions and exhaust gas temperature control of a heavy-duty diesel engine. International Journal of Engine Research, Vol. 21(8), pp. 1381-1397.

Hamedi, M. R., Doustdar, O., Tsolakis, A. & Hartland, J. (2019). Thermal energy storage system for efficient diesel exhaust aftertreatment at low temperatures. Applied Energy, Vol. 235, pp. 874-887.

Hoekstra, A. (2019). The underestimated potential of battery electric vehicles to reduce emissions. Joule, Vol. 3(6), pp. 1412-1414.

Honardar, S., Busch, H., Schnorbus, T., Severin, C., Kolbeck, A. F. & Korfer, T. (2011). Exhaust temperature management for diesel engines assessment of engine concepts and calibration strategies with regard to fuel penalty. SAE Technical Paper No. 2011-24-0176.

Hu, J., Wu, Y., Liao, J., Cai, Z. & Yu, Q. (2023). Heating and storage: A review on exhaust thermal management applications for a better trade-off between environment and economy in ICEs. Applied Thermal Engineering, Vol. 220, 119782.

Hushion, C., Thiruvengadam, A., Pondicherry, R., Thompson, G., Baltrucki, J., Janak, R., Lee, J., & Farrell, L. (2022). Investigating cylinder

deactivation as a low fuel-penalty thermal management strategy for heavy-duty diesel engines. Frontiers in Mechanical Engineering, Vol. 8, p. 987170.

Incropera, P., DeWitt, D., Bergman, T., & Lavine, A. (2007). Fundamentals of heat and mass transfer, John Wiley and Sons.

Jablonska, M. &Palkovits, R. (2016). Copper based catalysts for the selective ammonia oxidation into nitrogen and water vapour – recent trends and open challenges. Applied Catalysis B: Environmental, Vol. 181, pp. 332-351.

Jean, E. & Goncalves, M. (2023). Electrically Heated Catalyst: a powerful tool for aftertreatment optimization. SAE Technical Paper No. 2023-01-0351.

Jeyaseelan, T., Ekambaram, P., Subramanian, J., & Shamim, T. (2022). A comprehensive review on the current trends, challenges and future prospects for sustainable mobility. Renewable and Sustainable Energy Reviews, Vol. 157, 112073.

Joshi, M. C., Shaver, G. M., Vos, K., McCarthy Jr, J. & Farrell, L. (2022). Internal exhaust gas recirculation via reinduction and negative valve overlap for fuel-efficient aftertreatment thermal management at curb idle in a diesel engine. International Journal of Engine Research, Vol. 23(3), pp. 369-379.

Krishnamoorthi, M., Malayalamurthi, R., He, Z. & Kandasamy, S. (2019). A review on low temperature combustion engines: Performance, combustion and emission characteristics. Renewable and Sustainable Energy Reviews, Vol. 116, p. 109404.

Lee, D. H., Kim, H., Song, Y. H. & Kim, K. T. (2014). Plasma burner for active regeneration of diesel particulate filter. Plasma Chemistry and Plasma Processing, Vol. 34, pp. 159-173.

Lotus engineering software, Lotus Engine Simulation (LES) 2020 version. *Lotus Engineering*, Hethel, Norfolk.

Martinovic, F., Castoldi, L. & Deorsola, F. A. (2021). Aftertreatment technologies for diesel engines: An overview of the combined systems. Catalysts, Vol. 11, No. 6, p. 653.

Munnannur, A., Ottinger, N. & Gerald Liu, Z. (2022). Thermal Management of Exhaust Aftertreatment for Diesel Engines. In *Handbook of Thermal Management of Engines*, pp. 29-90. Springer, Singapore.

Nie, X., Bi, Y., Liu, S., Shen, L. & Wan, M. (2022). Impacts of different exhaust thermal management methods on diesel engine and SCR performance at different altitude levels. Fuel, Vol. 324, p. 124747.

Noor, C. M., Noor, M. M. & Mamat, R. (2018). Biodiesel as alternative fuel for marine diesel engine applications. Renewable and Sustainable Energy Reviews, Vol. 94, pp. 127-142.

Pachiannan, T., Zhong, W., Rajkumar, S., He, Z., Leng, X. & Wang, Q. (2019). A literature review of fuel effects on performance and emission characteristics of low-temperature combustion strategies, Applied Energy, Vol. 251, p. 113380.

Santos, N.D.S.A., Roso, V.R., Malaquias, A.C.T. and Baeta, J.G.C. (2021). Internal combustion engines and biofuels: Examining why this robust combination should not be ignored for future sustainable transportation. Renewable and Sustainable Energy Reviews, Vol. 148, p. 111292.

Scrosati, B., Garche, J. & Tillmetz, W. (2015). Advances in battery technologies for electric vehicles. Woodhead Publishing, pp. 8-11.

Shuzhan, B., Guobin, C., Qiang, S., Guihua, W. & Guo-xiang, L. (2017). Influence of active control strategies on exhaust thermal management for diesel particular filter active regeneration. Applied Thermal Engineering, Vol. 119, pp. 297-303.

Singh, A. P., Kumar, V. & Agarwal, A. K. (2020). Evaluation of comparative engine combustion, performance and emission characteristics of low temperature combustion (PCCI and RCCI) modes. Applied Energy, Vol. 278, p. 115644.

Soleimani, M., Campean, F. and Neagu, D. (2018). Reliability challenges for automotive aftertreatment systems: a state-of-the-art perspective. Procedia Manufacturing, Vol. 16, pp. 75-82.

Thangaraja, J. & Kannan, C. (2016). Effect of exhaust gas recirculation on advanced diesel combustion and alternate fuels-A review. Applied Energy, Vol. 180, pp. 169-184.

Truong, T. T., et al. (2021). Effect of alcohol additives on diesel engine performance: a review. Energy Sources, Part A: Recovery, Utilization, and Environmental Effects, pp. 1-25.

Vignesh, R. & Ashok, B. (2020). Critical interpretative review on current outlook and prospects of selective catalytic reduction system for De-NOx strategy in compression ignition engine. Fuel, Vol. (276), pp. 117996.

Wang, Z., Shen, L., Lei, J., Yao, G., & Wang, G. (2022). Impact characteristics of post injection on exhaust temperature and hydrocarbon emissions of a diesel engine. Energy Reports, Vol. 8, pp. 4332-4343.

Wardana, M. K. A. & Lim, O. (2022). Review of Improving the NOx Conversion Efficiency in Various Diesel Engines fitted with SCR System Technology. Catalysts, Vol. 13(1), p. 67.

Wei, H., Zhu, T., Shu, G., Tan, L., & Wang, Y. (2012). Gasoline engine exhaust gas recirculation-A review. Applied energy, Vol. 99, pp. 534-544.

Wu, B., Jia, Z., guo Li, Z., yi Liu, G., & lin Zhong, X. (2021). Different exhaust temperature management technologies for heavy-duty diesel engines with regard to thermal efficiency. Applied Thermal Engineering, Vol. 186, p. 116495

Xu, G. et al. (2023). Advances in emission control of diesel vehicles in China. Journal of Environmental Sciences, Vol. 123, pp. 15-29.

Zavala, B. A., McCarthy, J. E. & Harris, T. (2023). Burner Based Thermal Management Approach Utilizing In-Exhaust Burner Technology with CDA Equipped Engine, Frontiers in Mechanical Engineering, p. 124. Doi: 10.3389/fmech.2022.1022570.

Zhang, Z., Li, J., Tian, J., Dong, R., Zou, Z., Gao, S. & Tan, D. (2022). Performance, combustion and emission characteristics investigations on a diesel engine fueled with diesel/ethanol/n-butanol blends, Energy, Vol. 249, p. 123733.

Zhang, Z., Dong R., Lan, G., Yuan, T., & Tan, D. (2023). Diesel particulate filter regeneration mechanism of modern automobile engines and methods of reducing PM emissions: a review, Environmental Science and Pollution Research. https://doi.org/10.1007/s11356-023-25579-4.

CHAPTER 5

CORROSION PROPERTIES OF CuSnSi ALLOY IN DIFFERENT MEDIUMS

Dr. Ethem İlhan ŞAHİN[1]

Selim Burak CANTÜRK[2]

[1] Dr., Adana Alparslan Türkeş Bilim ve Teknoloji Üniversitesi, İleri Teknolojiler Uygulama ve Araştırma Merkezi, Adana, Türkiye. shnethem@gmail.com, ORCID ID :0000-0001-7859-9066
[2] Faculty of Mechanical Engineering, Slovak University of Technology, Námestie slobody 17, 812 31 Bratislava, Slovakia

1.INTRODUCTION

Due to its excellent resistance to corrosion, high electrical conductivity, tensile strength, resistance to wear, and appealing aesthetic appearance (which may be varied through the use of a number of alloying elements), copper has found broad employment in industrial settings (Alfantazi et al., 2009).

There are many different uses for copper and the alloys it may create, from electrical wire and electronic equipment to parts used in the transportation system.

Even though quite a bit of research on the subject of corrosion of copper alloys has been published (Mansfeld et all., 1994 ; Kear et all., 2004; Antonijevic and Petrovic 2008; Brusic et all., 1991; Wallinder et all., 2014), the focus of this research was solely on how different parameters affect corrosion. It has not been determined whether the corrosion process itself has any effect on the material's other qualities, such as its mechanical properties. Indeed, this knowledge is quite important fort he progree of copper alloys as well as the applications for which they are used.

The primary objective of this study is to get information of the resistance characteristics of copper alloy in various corrosive conditions. The changes that corrosive environments will cause in the microstructure of the alloy will be examined.

2. MATERIALS AND METHODS

2.1 Apparatus

Glass Beaker, pH meter, fish (polymer) net, %3.5 NaCI solution, Acidic&Alkaline solutions

Acidic Solution: 1 M , 50 ml HCI(weight p % 35 , d : 1.19 g/ml M.a : 36.46 g/mol)

Alkaline Solution: 1M , 50 ml NaOH (weight p % 98 , d : 2.13 g/ml M.a : 40.0 g/mol)

In the experimental procedure, copper alloys were sliced at a dimension of around 7.8 x 3.2 mm for diameter and thickness, respectively. The specimens was then mechanically polished by silicon carbide papers (sizes of 800 and 1200) and diamond paste (from 6 to 1 um) to make the smooth surface and remove physically attached impurities in the specimen.

After that, the polished specimens was washed with ethanol, rinsed with distilled water, wiped by a clean paper, and then dried at ambient temperature.

The corrosion test was done by putting and dipping the cleaned specimen in glass beakers containing different solutions. 3 different medium was picked for corrosion test and these are HCI, NaOH and NaCI. 1M solution of acid and alkaline was prepared with distilled water whereas %3.5 NaCI solution was picked since it is most common ratio for NaCI medium in the literature. The volumes of solution used for the immersion test was 50 ml (Figure 1). The corrosion test was done at a specific time from 1 to 3 weeks, which were performed at ambient temperature. Glass beakers was sealed hence there was no interaction between air (except the one already inside beaker). After the corrosion testing, the specimen was washed with distilled water, wiped by a clean paper, and stored in dessicator.

There are two samples used for each solution on this test. Samples are same, but one of each cleaned with H_2SO_4 to compare whether the cleaning product effect the weight loss. Samples 4,5 and 6 cleaned with H_2SO_4 on this experiment. Cleaning product is picked from the table for copper alloys on ISO/ DIS 8407 and ASTM G1-90 standarts.

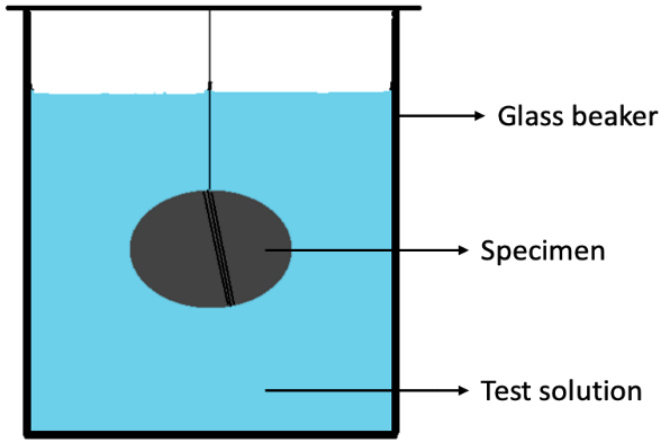

Figure 1: Illustration of immersion test.

3. RESULTS AND DISCUSSION

The specimens were withdrawn after period of exposure, the corrosion product removed, cleaned and the corrosion rate was determined. Results of weight loss after immersion test are given in table below. Results revealed that samples mostly damaged in the HCI medium in comparison to alkaline and neutral environment. In the NaOH and NaCI mediums specimens were not lost much weight. In addition, weight loss that comes from cleaning product is % 0.005 and it is also taken into account for samples 4, 5 and 6 (Table 1).

Table 1: Results of weight loss.

Samples No:	1	4 (H_2SO_4)	2	6 (H_2SO_4)	3	5 (H_2SO_4)
Corrosion Environment	HCI		NaCI		NaOH	
Diameter (mm)	7.84	7.82	7.85	7.80	7.83	7.80
Thickness(mm)	3.11	2.50	3.24	3.30	3.26	3.14
Initial weight(g) before corrosion	1.23591	1.00859	1.32151	1.38682	1.32260	1.29005
1 hour	1.23597	1.00852	1.32157	1.38694	1.32314	1.29030
6 hour	1.23583	1.00837	1.32142	1.38678	1.32236	1.28970
24 hour	1.23511	1.00802	1.32126	1.38671	1.32235	1.28956
48 hour	1.23455	1.00758	1.32126	1.38656	1.32228	1.28940

72 hour	1.23382	1.00702	1.32118	1.38641	1.32207	1.28928
96 hour	1.23281	1.00631	1.32110	1.38613	1.32183	1.28850
10 day	1.21708	0.99168	1.32044	1.38532	1.32104	1.28748
15 day	1.12214	0.89995	1.31954	1.38482	1.32091	1.28652
21 day	1.02804	0.81368	1.31881	1.38377	1.31964	1.28515

pH of corrosive mediums was also measured regularly each time weight losses was measured. XS 7 model portable pH meter used at this experiment. pH of the media is 7.5-8 for NaCl; It was around 13.3 for NaOH and finally about 0.3 for 1M HCl. Here, 1 M HCl was a high-grade acid, while 1M NaOH was again a highly alkaline medium. The 3.5% NaCl mixture, on the other hand, showed a near neutral basicity ratio.

The difference of samples can be seen from Figure 2. Initial samples had pale yellow-brownish color. After having exposed to corrosive mediums, there were color changes took place. The light colored samples are those that have been cleaned by the cleaning product. Also, it is observed that ultrasonic cleaning is much easier and faster after chemical cleaning. In this way, it is easy to get rid of the dirty layer on the surfaces. Surface tarneshing occurred in other samples in NaOH and NaCl solutions. In case of samples in HCI no tarnish was observed (Figure 2-3).

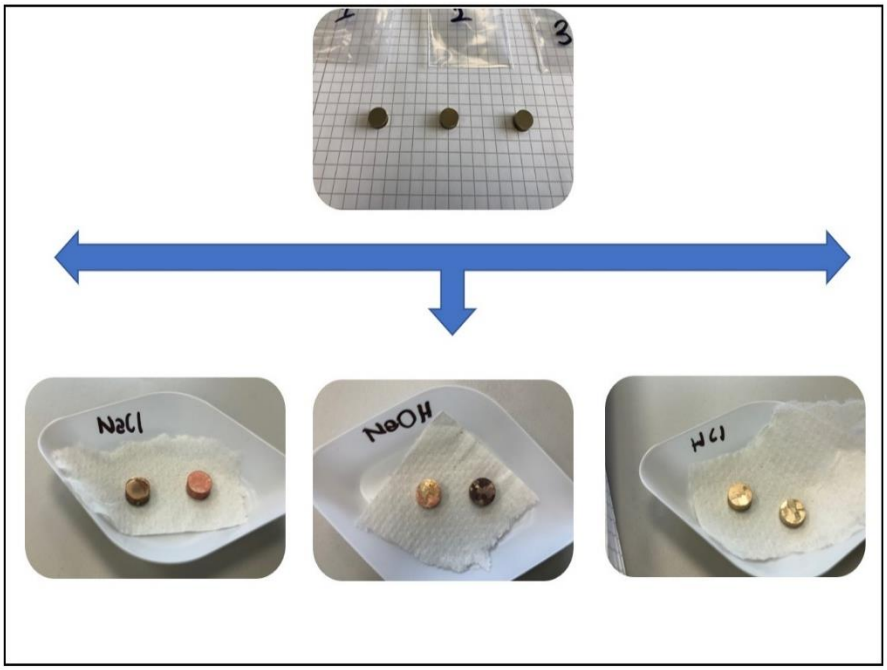

Figure 2: Images of surfaces before and after corrosion.

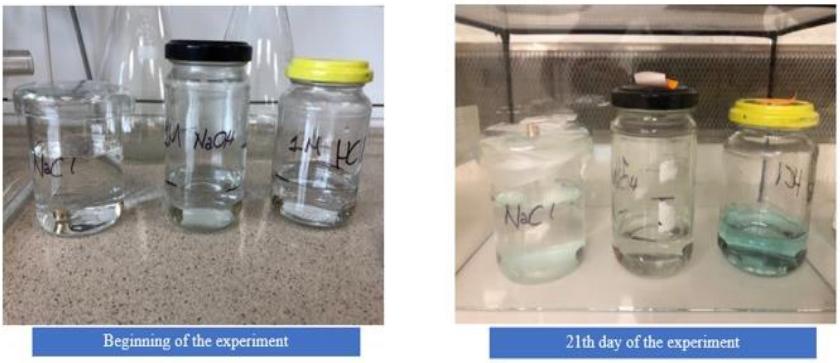

Figure 3: Images of corrosive mediums.

On 15th day, precipitation observed in NaCI solution and color of HCI solution began to turn blue. Pure copper is a very unreactive metal, and it does not react with pure hydrochloric acid. It is above copper in a metal reactivity series, so copper cannot replace the hydrogen. However, it reacts with dilute HCl to form copper chloride ($CuCl_2$) along with water (H_2O). The copper chloride formed is bluish-green in color, and being soluble in water, forms a light bluish-green solution. It is thought that's the reason behind color change in HCI medium. In another study, a similar color change observed (Elzey et all., 2011) . These changes did not significantly affect on pH of mediums.

Weight loss analysis is the most basic and well-established technique for calculating corrosion losses in machinery and other structures. A weighted sample (coupon) of the metal or alloy under examination is introduced to the process and later removed after a reasonable time interval. The voucher is then thoroughly cleansed of any corrosion-related substances and reweighed. The weight loss is transformed to a corrosion rate (CR) which can be calculated by the following equation;

$$\text{Corrosion rate} = (K \times W)/(A \times T \times D)$$

K= 8.76 x 10^4 mm per year

W= mass loss in g

A= area in cm^2 to the nearest 0.01 cm^2

T= time of exposure in hours

D= density in g/cm^3

A reference sample was used to determine the mass loss from cleaning and was subjected to the same cleaning procedure as the other samples. Result is % 0.005, and this value has been taken into account in the calculations.

Results are given in Table 2 below.

Table 2: Corrosion rate per year.

Sample No	K (constant)	W (mass loss) g	A (area) cm^2	T (exposure time) hour	D (density) g/cm^3	Corrosion Rate mm per year
1	87600	0.20787	1.731	504	8.23198	2.5348
2	87600	0.0027	1.767	504	8.42745	0.0315
3	87600	0.00296	1.765	504	8.42554	0.0346
4	87600	0.19491	1.575	504	8.39984	2.5611
5	87600	0.0049	1.725	504	8.59801	0.0574
6	87600	0.00305	1.764	504	8.79482	0.0342

Acidic solution shows the highest corrosion rate (2.5611 mpy), while alkaline and salt solutions were almost similar (average 0.3 mpy).

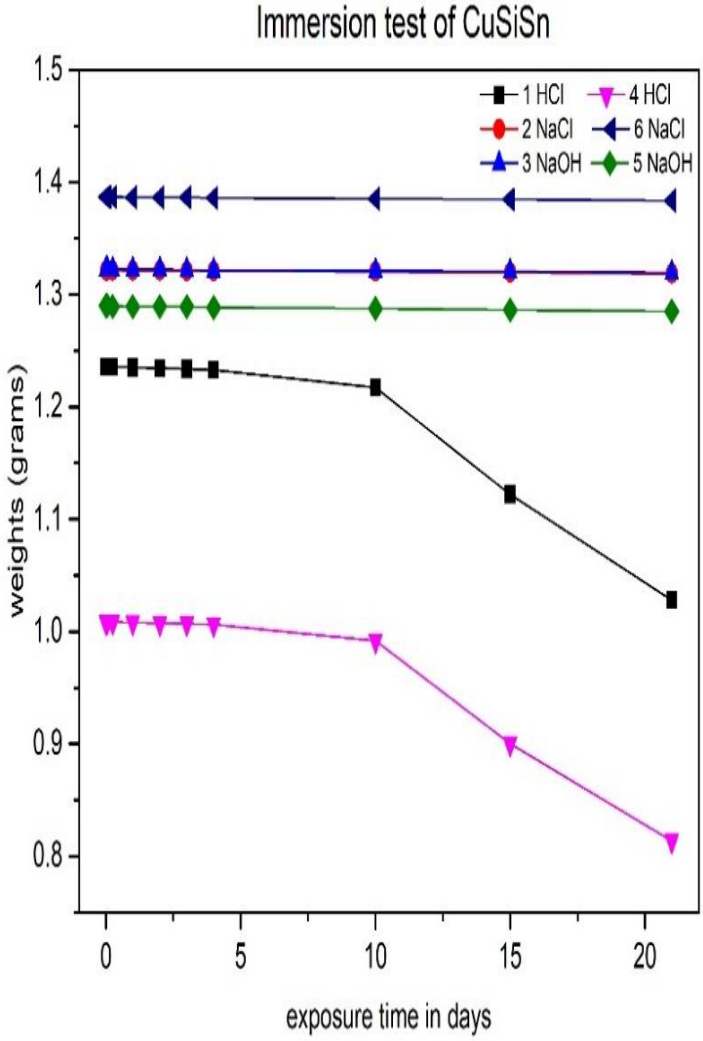

Figure 4: Changes in weight of samples in time.

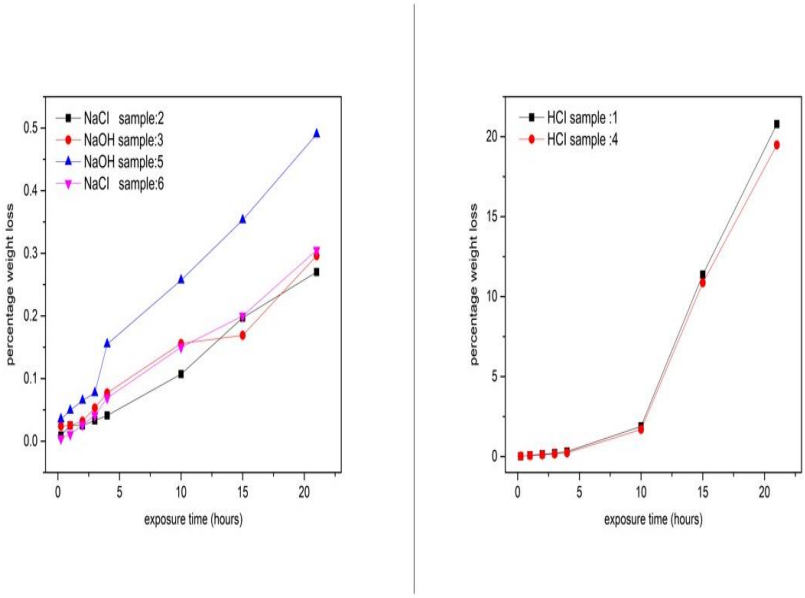

Figure 5: Percentage of weight loss versus time.

In the Figure 4, the mass losses experienced by the samples are given. As can be seen from the figure, the mass loss due to corrosion of samples in the NaOH and NaCl solutions rather low. On the other hand, significant mass losses occurred in the samples in HCl medium.

In order to see the difference better, mass losses were examined in percent and HCl was separated from other corrosive media. When we examine Figure 5, it is seen that the samples in the NaOH solutions experienced a mass loss between % 0.25-0.5. The samples in NaCl solution experienced mass losses of % 0.27-0.3. In case of samples in HCI medium, it is seen that there is a mass loss of around 20%. Also, Hydrochloric acid was triggered to increases in corrosion rates exponentially especially after 10^{th} days. As it will be remembered, samples 4, 5 and 6 were cleaned with H_2SO_4 chemical cleaning product. It is not possible to say anything definite about the effect of this cleaning procedure on the corrosion rate.

Looking at the graphs, while the corrosion rate is higher in samples 5 and 6, this rate is lower in sample 4 than the sample that is not cleaned with chemicals (Figure 5).

3.1. Microstructures

Microstructural examinations were made with both an optical microscope and SEM & EDS (Şahin 2023; Sahin et all., 2022; Topcu 2021). A reference sample was also examined prior to testing. SEM & EDS analyses were carried out with (Sahin 2022; Topcu 2020; Topcu et all., 2020) JEOL JSM-7600F model device.

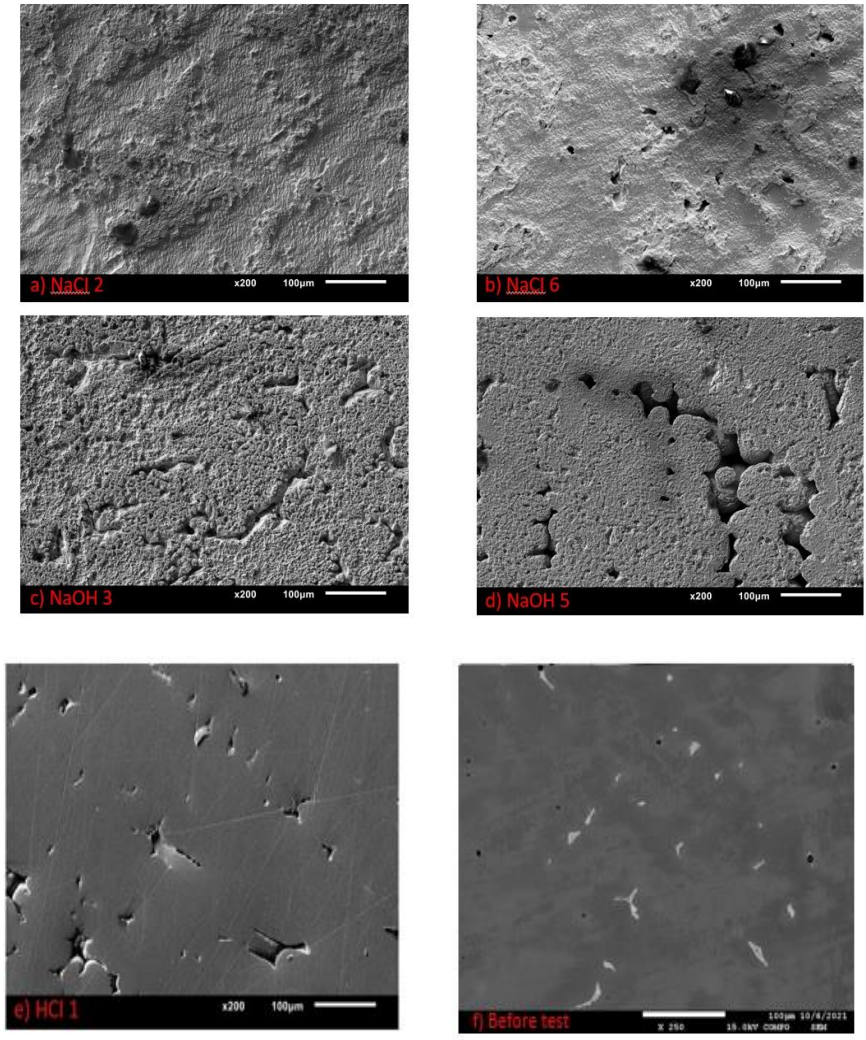

Figure 6: SEM images of samples.

Figure 6 reveals that corrosion forming for each sample by comparison with original sample. When the samples in NaOH medium are examined, it is stand out that the structure turns into a spongy state. In addition to a general deterioration in the structure, it was noticed that it contains large and small voids.

In case of samples in NaCI medium, corrosion generally appears to be distributed over the entire surface area. In addition to general attack corrosion, some cavities have also been observed.

In case samples in HCI, it is thought to be more like pitting corrosion than general corrosion. The cavities distributed throughout the microstructure were noticed. Optical microscope images are given alongside with the EDS results to see the general microstructures of the samples (figure 7).

HCI:1

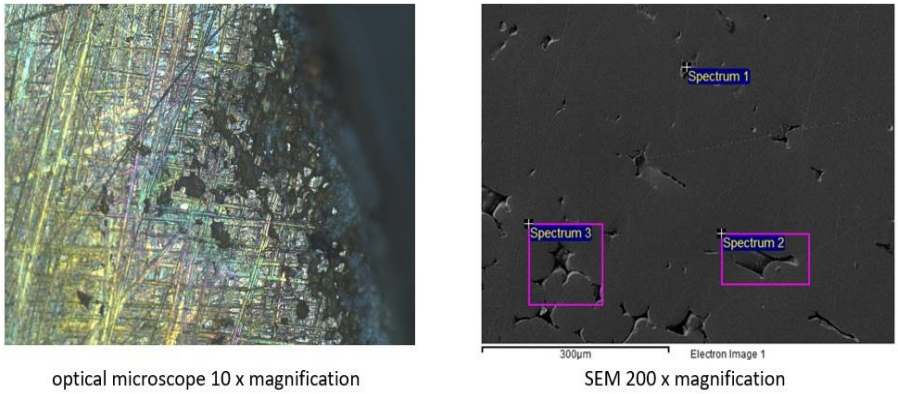

Figure 7: Optic and SEM images.

Table 3: Element content of selected locations.

Spectrum	In stats.	O	Si	Cu	Sn	Total
Spectrum 1	Yes		3.61	94.84	1.55	100.00
Spectrum 2	Yes	1.76	3.67	93.03	1.54	100.00
Spectrum 3	Yes	1.79	3.62	93.07	1.52	100.00
Max.		1.79	3.67	94.84	1.55	
Min.		1.76	3.61	93.03	1.52	

NaCI:2

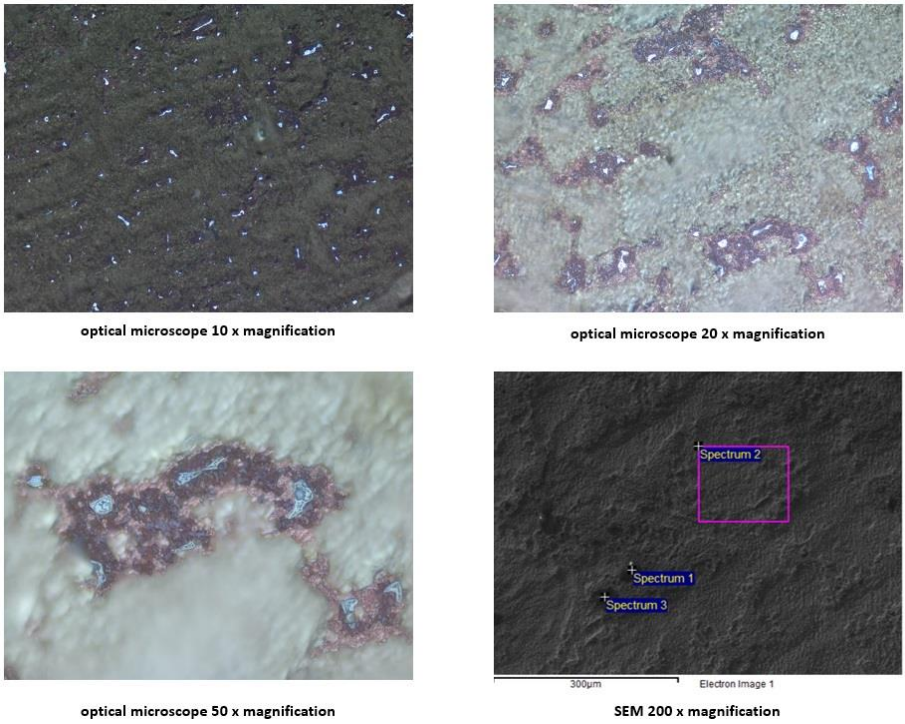

Figure 8: Optic and SEM images.

Table 4: Element content of selected locations.

Spectrum	In stat.	C	O	Na	Si	Cl	Cu	Sn	Total
Spectrum1	Yes	71.23	18.78	1.32		3.52	5.15		100.00
Spectrum 2	Yes		1.11		2.79		94.36	1.74	100.00
Max.		71.23	18.78	1.32	2.79	3.52	94.36	1.74	
Min.		71.23	1.11	1.32	2.79	3.52	5.15	1.74	

NaCI:6

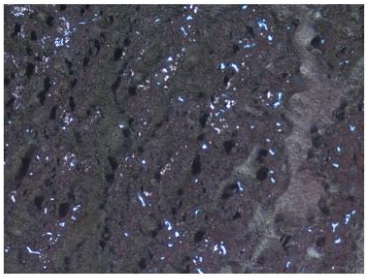

optical microscope 10 x magnification

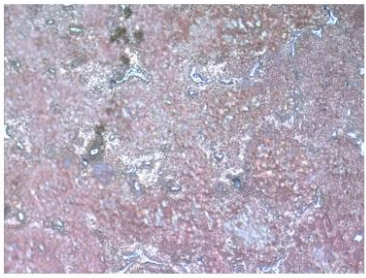

optical microscope 20 x magnification

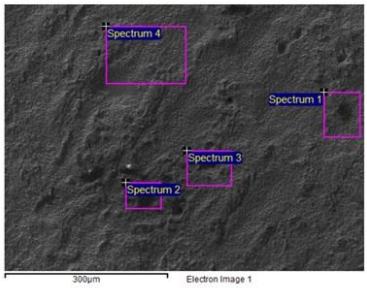

SEM 200 x magnification

Figure 9: Optic and SEM images.

Table 5: Element content of selected locations.

Spectrum	In stats.	C	O	Si	Cu	Sn	Total
Spectrum 1	Yes	17.13	2.34	1.33	78.13	1.08	100.00
Spectrum 2	Yes	32.73	4.09	0.89	62.29		100.00
Spectrum 3	Yes		0.59	1.51	96.71	1.19	100.00
Spectrum 4	Yes	6.60	0.76	1.73	89.63	1.28	100.00
Max.		32.73	4.09	1.73	96.71	1.28	
Min.		6.60	0.59	0.89	62.29	1.08	

NaOH: 3

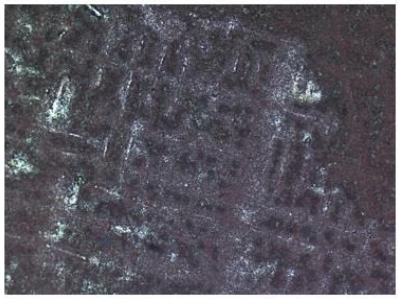

optical microscope 10 x magnification

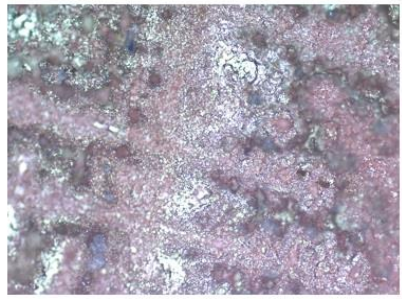

optical microscope 20 x magnification

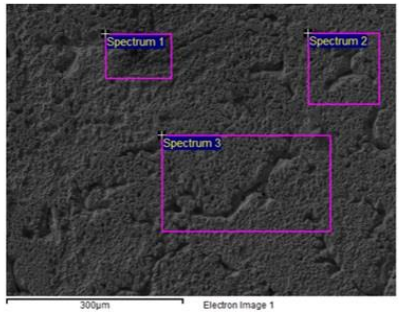

SEM 200 x magnification

Figure 10: Optic and SEM images.

Table 6: Element content of selected locations.

Spectrum	In stats.	O	Si	Cu	Sn	Total
Spectrum 1	Yes	2.25	2.01	94.27	1.48	100.00
Spectrum 2	Yes	1.18	2.16	95.30	1.37	100.00
Spectrum 3	Yes	1.14	2.05	95.24	1.57	100.00
Mean		1.52	2.07	94.94	1.47	100.00
Std. deviation		0.63	0.08	0.58	0.10	
Max.		2.25	2.16	95.30	1.57	
Min.		1.14	2.01	94.27	1.37	

NaOH: 5

optical microscope 10 x magnification

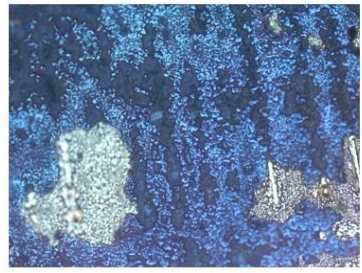

optical microscope 20 x magnification

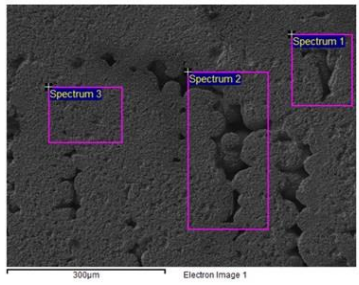

SEM 200 x magnification

Figure 11: Optic and SEM images.

Table 7: Element content of selected locations.

Spectrum	In stats.	O	Cu	Total
Spectrum 1	Yes	12.58	87.42	100.00
Spectrum 2	Yes	12.71	87.29	100.00
Spectrum 3	Yes	12.43	87.57	100.00
Mean		12.57	87.43	100.00
Std. deviation		0.14	0.14	
Max.		12.71	87.57	
Min.		12.43	87.29	

In general, results exhibits SEM images of copper alloy samples after corrosion testing, with particular focus on voids in the structure, to confirm the visual observations in the optical microscope results. Figure 7-11 is the optical and SEM images of the samples under HCl, $NaCl_2$, $NaCl_6$ and $NaOH_3$ and $NaOH_5$, respectively.

As seen in the SEM analysis images, there is general deteriorations in some microstructures, as well as voids (as black areas). To confirm the elemental composition of the corroded samples, EDS analysis was performed in the black pitting areas. The results confirmed that there was oxygen formation in the black pitting areas in all samples. This indicates that those areas are corroded. In addition, oxygen formation is observed in areas where there are no pits. This can be interpreted as general corrosion formation. In the $NaCl_2$ sample, apart from oxygen, Na and Cl elements were also detected on the surface area.

4. CONCLUSION

The corrosion characteristics of copper alloys were successfully examined after immersion for 21 days in different solutions (NaOH, HCl and NaCl) with various concentrations (1M, 1M and 3.5 %). The pH values for corrosive mediums (NaOH, HCI and NaCI) were 13.3, 0.3 and 7.5 respectively. There was no significant change on pH values at the end of experiment. During experiments 2 samples used for same corrosive mediums. One of each was cleaned with dilute H_2SO_4 solution according to ASTM G1-90 standard. Also a reference sample is cleaned with cleaning product to calculate the mass loss from this procedure and result was added in to total mass loss for samples 4, 5 and 6. Samples that cleaned with H_2SO_4 had more light color surface and it was easier to cleaned after experiment.

Corrosion rates were calculated in terms of mm per year. According to result, samples in which in NaCI and NaOH mediums had shown around % 0.3-0.5 mass loss. On the other hand, samples that immersed in HCI medium had experienced around % 20 mass loss. This indicate that samples lost almost 40 times more mass in HCI. The mass loss that comes from cleaning product had not shown any pattern. Therefore, effect is not clear.

SEM and surface analysis showed that corrosion is appears to be general in all samples, also in HCI samples, corrosion seems more like pitting alongside with general deterioration. EDS results confirm that oxygen formed on the pitting areas pointing the main rust is CuO. Cavities are darker and

larger in HCI in comparison to the ones in NaOH and NaCI. This might verify that corrosion is much more in HCI.

All the Results exhibit that CuSiSn alloy highly resistant to salt and NaOH corrosive mediums. However, this alloy had shown major mass loss in HCI medium. Hence, it can be state that HCI corrosive medium is considerably hazardous for this alloy.

5. ACKNOWLEDGE

In honor of Prof. Ayhan MERGEN, who passed away in 2017, this work was made. For their assistance, we also acknowledge Marmara University, Adana Alparslan Türkeş Science and Technology University and İstanbul Technical University.

REFERENCES

Alfantazi AM, Ahmed MTM, Tromans D. Corrosion behavior of copper alloys in chloride media. Mater. Des. 2009: 30 (7); 2425–2430.

Antonijevic MM, Petrovic MB. Copper corrosion inhibitors. A review, Int. J. Electrochem. Sci. 2008: 3 (1); 1–28.

Brusic V, Frisch MA, Eldridge BN, Novak FP, Kaufman FB, Rush BM, Frankel GS. Copper corrosion with and without inhibitors. J. Electrochem. Soc. 1991: 138 (8); 2253–2259.

Elzey S, Baltrusaitis J, Bian S, and Grassian VH. Formation of paratacamite nanomaterials *via* the conversion of aged and oxidized coppernanoparticles in hydochloric acidic media. J. Mater. Chem. 2011: 21; 3162-3169.

Kear G, Barker BD, Walsh FC. Electrochemical corrosion of unalloyed copper in chloride media—a critical review. Corros. Sci. 46 (1) (2004) 109–135.

Mansfeld F, Liu G, Xiao H, Tsai CH, Little BJ. The corrosion behavior of copper alloys, stainless steels and titanium in seawater. Corros. Sci. 1994: 36 (12); 2063–2095.

Sahin Eİ, Microwave electromagnetic shielding effectiveness of $ZnNb_2O_6$-chopped strands composites for radar and wideband (6.5-18 GHz) applications. Lithuanian Journal of Physics 2022: 62 (3); 161-170.

Şahin Eİ, Emek M, Ibrahim JEFM, Fizik ve Matematik Alanında Akademik Çalışmalar. Prof. Dr. Elif Orhan, Dr. Öğr. Üyesi Elanur Seven, İksad Publishing House. 2022: 121-132.

Şahin Eİ, Electromagnetic shielding effectiveness of $Ba(Zn_{1/3}Nb_{2/3})O_3$:Chopped strands composites for wide frequency applications. Journal of Ceramic Processing Research 2023: 24(1); 1-7.

Topcu İ, Mechanical properties of PLA and ABS parts produced with fused filament fabrication method. Journal of Ceramic Processing Research 2021: 22 (2); 143–148.

Topcu İ, Investigation of wear behavior of particle reinforced AL/B4C composites under different sintering conditions, Tehnicki Glasnik 2020: 14(1); 7-14.

Topcu İ, Ceylan M, Yılmaz EB. Experimental investigation on mechanical properties of multi wall carbon nanotubes (MWCNT) reinforced aluminium metal matrix composites, Journal of Ceramic Process Research 2020: 21(5); 596-601.

Wallinder, IO, Zhang X, Goidanich S, Bozec L, Herting N, Leygraf G-C. Corrosion and run off rates of Cu and three Cu-alloys in marine environments with increasing chloride deposition rate. Science of the total environment 2014: 472, 681-694.

ISBN: 978-625-367-000-9